Journal of Materials Chemistry B

PAPER

View Article Online
View Journal | View Issue

Cite this: J. Mater. Chem. B, 2020, 8, 226

A self-healable and antifouling hydrogel based on PDMS centered ABA tri-block copolymer polymersomes: a potential material for therapeutic contact lenses†

Sovan Lal Banerjee, Sarthik Samanta, Shrabana Sarkar and Nikhil K. Singha *

Received 11th May 2019,
Accepted 1st November 2019

DOI: 10.1039/c9tb00949c

rsc.li/materials-b

Herein we have prepared an antifouling and self-healable poly(dimethyl siloxane) (PDMS) based hydrogel which consists of a mixture of curcumin loaded zwitterionic PDMS polymersomes and amine functionalized PDMS polymersomes prepared *via* Reversible Addition–Fragmentation Chain Transfer (RAFT) polymerization and a Schiff-base reaction. The curcumin loaded polymersome consists of a PDMS and poly([dimethyl-[3-(2-methyl-acryloylamino)-propyl]-(3-sulfopropyl)ammonium)] (poly(sulfobetaine)) based tri-block copolymer (BCP) and it was characterized by dynamic light scattering (DLS), high resolution transmission electron microscopy (HRTEM), field emission scanning electron microscopy (FESEM) and atomic force microscopy (AFM) analyses. To prepare the hydrogel, amine functionalized PDMS polymersomes were crosslinked with polyethylene glycol dialdehyde (PEG-DA) in pH 7.4 buffer solution *via* a Schiff-base reaction. This hydrogel was able to show sustained delivery of the entrapped curcumin drug for more than 72 h. The self-healing characteristic of the prepared hydrogel in the presence of saline water was elucidated by the "scratch and heal" method and subsequently analyzed through tensile study. Due to the presence of the poly(zwitterionic) moiety in the hydrogel system, it was observed that the hydrogel can efficiently reduce protein deposition, where Bovine Serum Albumin (BSA) was taken as a model protein. It was observed that the curcumin loaded hydrogel was detrimental towards both Gram-negative (*Escherichia coli*) and Gram-positive (*Staphylococcus aureus*) bacteria. This type of smart soft hydrogel system can be a potential material for therapeutic applications for several eye diseases.

1. Introduction

In recent days, soft contact lenses (SCL) have been extensively used for improving a wide range of vision deficiencies. A high level of drug loading, controlled release of the therapeutics, wearing comfort, and ease of removal from the ocular surface are the major advantages of using soft hydrogel based contact lenses.[1,2] Since the invention of the first soft hydrogel contact lenses based on poly(2-hydroxyethyl methacrylate) (PHEMA) (having 38% water content) by Lim and Otto, there has been a plethora of literature in this field.[3] Among 150 different types of available soft contact lenses, PHEMA has been the most widely used material. But the poor permeation of oxygen of the conventional PHEMA based hydrogel provokes the development of silicone based SCL, which dramatically improve the corneal oxygen supply (commercially available since 1999).[4] The presence of the silicone domain offers least resistance to oxygen permeation through the hydrogel system, which positively reduces hypoxia related complications. Apart from the oxygen permeation, PDMS based SCL provide transparency, good biocompatibility, and thermal and oxidative stability. For this reason it is reported that silicone based SCL are appropriate for developing artificial ophthalmic devices like contact lenses, soft intraocular lenses, artificial corneas *etc.*[5–7] In this work, we have designed a smart PDMS based SCL with an encapsulated antimicrobial and antifouling agent to fight against microbial infection as well as to reduce biofilm formation. It is a well-reported fact that microbial infections in the eyes can result in blindness and morbidity. To fight against these types of fungal and microbial diseases, generally, intraocular injection or eye drops are used for specific delivery of the drug and to reduce drug induced side effects.[8,9] But the problems associated with this type of system are poor solubility and dispersity of the drug molecules, which result in poor bioavailability of the drugs. It is reported that only 1–7% of the applied dosage reaches the targeted site as the rest of the

Rubber Technology Centre, Indian Institute of Technology, Kharagpur 721302, India. E-mail: nks8888@yahoo.com, nks@rtc.iitkgp.ernet.in

† Electronic supplementary information (ESI) available: Characterization, synthesis procedure of the PDMS based macro-RAFT reagent, characterization data (NMR, FTIR, AFM, GPC, contact angle, optical microscope image and tensile test) for the compounds. See DOI: 10.1039/c9tb00949c

applied drug is washed out with the tears due to eye movement.[10] So, the patient has to be administered the drug several times in a day. As a consequence, the use of drug loaded soft hydrogel based contact lenses is the best alternative for the sustained delivery of the entrapped drug molecules, particularly in the case of fungal infections like fungal keratitis infection where formation of a strong biofilm resists the penetration of eye drops.[11,12]

The major limitations associated with hydrophobic PDMS based SCL are poor wettability, and excessive deposition of proteins (such as lactoferrin, lysozyme and albumin), mucin and lipids, which impart several ocular discomforts.[13] To optimize the required hydrophilicity in PDMS based hydrogels, in many cases the PDMS surface is modified to ensure good wettability *via* stabilization of the tear film over and under the contact lens.[14] Bozukova *et al.*,[15] Chen *et al.*[16] and many other researchers have reported the effect of PEG in other polymer compositions to incorporate hydrophilicity and anti-protein adhesion properties. Deposition of certain proteins results in an increase in the generation of microbes that can accelerate inflammatory related complications like giant papillary conjunctivitis.[17] The problem associated with PEG is its auto-oxidative nature to form ether and aldehyde, resulting in the loss of the antifouling activity of PEG.[18] This limitation associated with the PEG polymer provokes the emergence of a new class of polymeric material that can resist protein deposition as well as stay strong against the chemical degradation process. Jiang and co-workers reported that poly(zwitterionic) materials (poly(sulfobetaine)), poly(carboxybetaine) and poly(phosphobetaine) can show ultralow-fouling, salt-resistance properties (anti polyelectrolyte effect), excellent hydrophilicity and biocompatibility.[19,20]

The major objective of this investigation is to prepare a new PDMS based hydrogel having a hydrophilic zwitterionic moiety and to use this material for effective delivery of hydrophobic drugs like curcumin, a natural drug as a model. Curcumin has a composition of 1,7-bis-(4-hydroxy-3-methoxyphenyl)-1,6-heptadiene-3,5-dione and can exist in both keto (in neutral as well as acidic solution) and enol (in alkaline media) tautomeric forms.[21] It is approved as a "generally regarded as safe" compound by the U.S. Food and Drug Administration.[22] Curcumin is a multi-functional drug that can efficiently control different diseases like anterior segment eye diseases, *e.g.* oxidative stress, inflammation due to conjunctivitis, hyperglycemia, glucoma *etc.*[23] But the use of curcumin in ocular delivery is restricted due to its lower bio-availability, as it is poorly soluble in water.[23] In this case, we have prepared a unique PDMS based polymersome system where the middle block of the polymersome forming ABA triblock copolymer is hydrophobic in nature (B segment, PDMS block), which helps in encapsulating the hydrophobic drug *via* hydrophobic–hydrophobic interactions. The outer hydrophilic layer (A segment, polyzwitterionic block) helps the polymersome to easily disperse into the hydrophilic hydrogel system as well as to increase the bioavailability of the hydrophobic drug. Polymersomes are a class of polymeric materials having a diameter of 50 nm to 5 μm prepared using amphiphilic synthetic block copolymers.[24] Polymersomes can exist in the form of vesicular structures or in the form of hollow tubes that can encapsulate water.[25]

In this application, the hydrogel should have self-healing properties apart from the antifouling characteristics so that the structural integrity of the contact lens will be maintained in the event of any damage or cracks during the usage of this material. In this case, we have studied the self-healing characteristics of the hydrogel after the generation of artificial micro cracks. There have been several approaches to prepare self-healable polymer materials, such as based on Diels–Alder reactions,[26,27] disulfide reactions,[28,29] ionic interactions[30] *etc.* Here, we have utilized a simple ionic interaction approach that can provide dynamic self-healing instantaneously and repeatedly.

This investigation reports the preparation of a PDMS centered tri-block copolymer based soft hydrogel material *via* xanthate mediated RAFT polymerization and a Schiff-base reaction. The hydrogel consists of PDMS based polyzwitterionic polymersomes and polyethylene glycol dialdehyde (CHO–PEG–CHO) crosslinked amine functionalized PDMS polymersomes. To prepare the amine functionalized PDMS, a poly(glycidyl methacrylate)-*block*-polydimethylsiloxane-*block*-poly(glycidyl methacrylate) (PGMA-*b*-PDMS-*b*-PGMA) triblock copolymer was prepared using RAFT–PDMS–RAFT as a macro RAFT reagent followed by the amination of the PGMA unit using ethylene diamine (EDA) as a ring opening reagent for the glycidyl group of the PGMA unit. This tri-block copolymer was crosslinked *via* a Schiff-base reaction. To incorporate self-healing, antifouling and antimicrobial properties, during the crosslinking reaction a curcumin incorporated PDMS based zwitterionic polymersome was added into the system. The PDMS based zwitterionic BCPs were synthesized *via* a sequential copolymerization method where RAFT–PDMS–RAFT was used as a macro RAFT reagent to prepare the second block of poly(*N*-[3-(dimethylamine)propyl]methacrylamide) (PDMAPM-*b*-PDMS-*b*-PDMAPM) followed by its betainization using 1,3-propane sultone *via* a ring opening reaction. To the best of our knowledge, the preparation of this type of PDMS hydrogel based on covalent as well as zwitterionic interactions and its application in therapeutic contact lenses have not been reported so far.

2. Experimental

2.1. Materials

Poly(dimethylsiloxane), bis(hydroxyalkyl) terminated (M_n = 5600 g mol^{-1}) (OH–PDMS–OH), *N*-[3-(dimethylamine)propyl]-methacrylamide (DMAPM), glycidyl methacrylate (GMA), 1,3-propanesultone, 2-bromopropionyl bromide (97%) (BPBr), triethylamine (Et_3N), 4,4′-azobis (4-cyanovaleric acid) (ABCVA) (thermal initiator), carbon disulfide (CS_2), diethyl ether (Et_2O), potassium hydroxide (KOH), ethanol (EtOH), *N*,*N*′-dicyclohexylcarbodiimide (DCC), 4-(dimethylamino)pyridine (DMAP), 4-formyl benzoic acid (FBA), dichloro methane (CH_2Cl_2, DCM), anhydrous magnesium sulfate ($MgSO_4$) and sodium hydrogen carbonate ($NaHCO_3$), ethylene diamine (EDA), curcumin (Cur) drug, and bovine serum albumin (BSA) were purchased from Sigma-Aldrich, USA.

2.2. Methods

The preparation of the PDMS based macro-RAFT reagent has been explained in the ESI.†

2.2.1. Synthesis of the tri-block copolymer of poly(*N*-[3-(dimethylamino)propyl]methacrylamide) (PDMAPM-*b*-PDMS-*b*-PDMAPM) using RAFT–PDMS–RAFT as a macro-RAFT reagent. In a typical xanthate mediated RAFT polymerization process,[30–34] PDMS macro RAFT ($M_{n/GPC}$ = 6000 g mol^{-1}) (0.98 g, 1.63 × 10^{-4} mol) was dissolved in 1.5 ml of DMF in a Schlenk tube under inert (N_2 atm) conditions. After that, the monomer DMAPM (4.2 g, 2.4 × 10^{-2} mol) and a DMF solution of the thermal initiator ABCVA (0.012 g, 4.28 × 10^{-5} mol) (0.5 ml) were purged into the Schlenk tube (Table 1). The reaction mixture was allowed to stir for 30 min under an inert atmosphere and after that the whole system was transferred to an oil bath having a temperature of 80 °C. After 24 h, the Schlenk tube was placed into an ice bath to terminate the reaction followed by the precipitation of the obtained product in diethyl ether. Finally, the tri-block copolymer PDMAPM-*b*-PDMS-*b*-PDMAPM was acquired *via* drying in a vacuum oven for 48 h at 40 °C (for $PDMAPM_{73}$-*b*-$PDMS_{65}$-*b*-$PDMAPM_{73}$ (conversion = 98%, $M_{n/GPC}$ = 30 500 g mol^{-1}, $Đ$ = 1.34)) [^{1}H NMR, $CDCl_3$, δ = 0.07 ppm (Si-C**H**$_3$), δ = 0.56 ppm (Si-C**H**$_2$-CH$_2$–), δ = 1.64 ppm (Si-CH$_2$-C**H**$_2$–), δ = 1.66 ppm (C**H**$_3$-CH$_2$-O–), δ = 2.29–2.33 ppm (–N-(C**H**$_3$)$_2$ and (CH$_3$)$_2$-N-C**H**$_2$–), δ = 3.20 ppm (–CO-NH-C**H**$_2$–), δ = 3.55–3.45 ppm (–C**H**$_2$-O–) and δ = 4.66 ppm (**i**, CH$_3$-C**H**$_2$-O–)].

2.2.2. Synthesis of zwitterionic block copolymer (ZPDMAPM-*b*-PDMS-*b*-ZPDMAPM) *via* betainization of the PDMAPM-*b*-PDMS-*b*-PDMAPM copolymer. The betainization of the PDMS based tri-block copolymer (PDMAPM-*b*-PDMS-*b*-PDMAPM) was carried out by a ring opening reaction of 1,3-propane sultone to prepare the zwitterionic block copolymer. In a typical synthesis process, a 50 wt% excess of 1,3-propane sultone (1.5 g, 1.23 × 10^{-2} mol) and the tri-block copolymer PDMAPM-*b*-$PDMS_{65}$-*b*-PDMAPM (1 g, 3.27 × 10^{-5} mol) were dissolved in 25 ml of dry THF and the reaction mixture was allowed to stir for 24 h at room temperature. After that, THF was distilled out using a rotary-evaporator and the obtained product was dissolved in a minimum volume of water followed by re-precipitation from excess THF. The precipitate was collected *via* centrifugation and subsequent drying under a vacuum at 30 °C. ^{1}H NMR of the product was carried out using D_2O as a solvent to confirm the formation of the zwitterionic polymer [^{1}H NMR, D_2O, δ = 0.07 ppm (Si-C**H**$_3$), δ = 0.56 ppm (Si-C**H**$_2$-CH$_2$–), δ = 1.64 ppm (Si-CH$_2$-C**H**$_2$–), δ = 1.66 ppm (C**H**$_3$-CH$_2$-O–), δ = 2.94 ppm (–C**H**$_3$-SO$_3^-$), δ = 3.10 ppm ([–N(CH$_2$)(C**H**$_3$)$_2$]$^+$), δ = 3.46 ppm ([–N(C**H**$_2$)(CH$_3$)$_2$]$^+$), δ = 3.55–3.45 ppm (–C**H**$_2$-O–) and δ = 4.66 ppm (CH$_3$-C**H**$_2$-O–)].

2.2.3. Synthesis of the tri-block copolymer of poly(glycidyl methacrylate) (PGMA-*b*-PDMS-*b*-PGMA) using RAFT–PDMS–RAFT as a macro-RAFT reagent. In a typical polymerization method, PDMS macro RAFT ($M_{n/GPC}$ = 6000 g mol^{-1}) (0.98 g, 1.6 × 10^{-4} mol) was dissolved in 1.5 ml of DMF in a Schlenk tube under inert (N_2 atm) conditions for 10 min. After that, a DMF solution of GMA (4.4 g, 3.1 × 10^{-2} mol) and the thermal initiator ABCVA (0.012 g, 4.25 × 10^{-5} mol) (dissolved in 0.5 ml of DMF) were injected into the Schlenk tube under a nitrogen atmosphere (Table 1). The reaction mixture was stirred under N_2 conditions for 30 min and then placed into an oil bath kept at 80 °C to carry out the polymerization reaction for 24 h. After completion of the reaction, the reaction was quenched by placing the Schlenk tube into cold water. The product ($PGMA_{93}$-*b*-$PDMS_{65}$-*b*-$PGMA_{93}$) was obtained after precipitation in diethyl ether followed by drying in a vacuum oven at 40 °C (conversion = 98%, $M_{n/GPC}$ = 32 000 g mol^{-1}, $Đ$ = 1.42) [^{1}H NMR, $CDCl_3$, δ = 0.07 ppm (Si-C**H**$_3$), δ = 0.56 ppm (Si-C**H**$_2$-CH$_2$–), δ = 1.64 ppm (Si-CH$_2$-C**H**$_2$–), δ = 1.66 ppm (C**H**$_3$-CH$_2$-O–), δ = 2.65 ppm and 2.86 ppm (–C**H**$_2$-O-CH–), δ = 3.55–3.45 ppm (–C**H**$_2$-O–), δ = 3.25 ppm (–CH$_2$-O-C**H**–), δ = 3.84 ppm and 4.31 ppm (–COO-C**H**$_2$–) and δ = 4.66 ppm (CH$_3$-C**H**$_2$-O–)].

2.2.4 Amine modification of the tri-block copolymer. For the amination of the tri-block copolymer PGMA-*b*-PDMS-*b*-PGMA, a predetermined amount of the block copolymer (2.5 g, 7.8 × 10^{-5} mol) was dissolved in DMF (30 ml) in a 100 ml round-bottomed flask and purged with nitrogen for 10 min to make the inner atmosphere inert. After that, the whole system was transferred to an oil bath kept at 80 °C. Approximately, a 3 mol% excess of ethylene diamine (1 ml) was added dropwise to the system using a dropping funnel under continuous stirring conditions for 15 min, maintaining the inert atmosphere. After completion of the reaction, the ethylene diamine modified block copolymer was precipitated out in excess diethyl ether. The obtained product was again dissolved in DMF and then dialyzed in deionized water using a dialysis tube having a molecular weight cut off of 3 kDa. After that, the dialyzed solution was freeze-dried to get the amine modified PGMA-*b*-PDMS-*b*-PGMA (AmPGMA-*b*-PDMS-*b*-AmPGMA) [δ = 0.07 ppm (Si-C**H**$_3$), δ = 0.56 ppm (Si-C**H**$_2$-CH$_2$–), δ = 1.64 ppm (Si-CH$_2$-C**H**$_2$–), δ = 1.66 ppm (C**H**$_3$-CH$_2$-O–), δ = 2.79 ppm (–NH-C**H**$_2$-C**H**$_2$-NH$_2$), δ = 2.91 ppm (–CH-C**H**$_2$-NH–), δ = 3.13 ppm (–C**H**-OH), δ = 3.55–3.45 ppm (–C**H**$_2$-O–) and δ = 4.66 ppm (CH$_3$-C**H**$_2$-O–)].

2.2.5. Synthesis of polyethylene glycol-dialdehyde. Polyethylene glycol-dialdehyde (PEG-DA) was prepared by the modification of PEG using 4-formyl benzoic acid (FBA) *via* a Steglich

Table 1 Different BCPs *via* xanthate mediated RAFT polymerization using modified PDMS as a macro-RAFT reagent[a] in DMF at 80 °C

Expt. no.	Sample composition	[M] : CTA-RAFT : [I]	Conv. (%)	$M_{n/NMR}$ (g mol^{-1})	$M_{n/GPC}$ (g mol^{-1})	$Đ$	$M_{n/Theo}$ (g mol^{-1})
1	$PDMAPM_{73}$-*b*-$PDMS_{65}$-*b*-$PDMAPM_{73}$	584 : 4 : 1	98	24 500	30 500	1.34	30 856
2	$PGMA_{93}$-*b*-$PDMS_{65}$-*b*-$PGMA_{93}$	744 : 4 : 1	98	28 600	32 000	1.42	32 440

[a] RAFT polymerization of DMAPM and PGMA was carried out using xanthate modified PDMS of M_n = 6000 g mol^{-1} as a macro-RAFT reagent in DMF at 80 °C.

esterification reaction. In a typical synthesis method, PEG-4000 (5 g, 1.25×10^{-3} mol), FBA (1.5 g, 10×10^{-3} mol) and DMAP (3 g, 2.46×10^{-2} mol) were mixed in 40 ml of dry THF and allowed to stir for 1 h at ice cold temperature. After that, a dry THF solution of DCC (5.159 g, 2.5×10^{-2} mol) was added dropwise to the prepared solution for 15 min under vigorous stirring conditions under an inert atmosphere (N_2 atm). The reaction mixture was allowed to stir at room temperature for 48 h followed by the centrifugation of the obtained solution to remove the insoluble dicyclohexyl urea (DCU). The obtained supernatant was concentrated using a rotary-evaporator and was precipitated out in diethyl ether. The precipitate was again re-dissolved in 5 ml of THF and subjected to dialysis against deionized water using a dialysis membrane having a molecular weight cut off of 3 kDa for 24 h. The deionized water was replaced with fresh every 12 h. The final product after dialysis was obtained *via* the freeze drying process and analyzed using $CDCl_3$ as a solvent (δ = 3.86 ppm (**a**, –O-C**H**$_2$-C**H**$_2$-O–), δ = 7.96 ppm (**c**, CHO-phenyl ring proton), δ = 8.22 ppm (**b**, –COO-phenyl ring proton), δ = 10.12 ppm (–C**H**O)).

2.2.6. Preparation of the PDMS hydrogel *via* a Schiff-base reaction. In a typical preparation method, 10 ml of an aqueous solution of (concentration 300 mg ml^{-1}) the AmPGMA-*b*-PDMS-*b*-AmPGMA polymersome was mixed with 5 ml of an aqueous solution of polyethylene glycol-dialdehyde (concentration 100 mg ml^{-1}) in a reaction tube and homogenized for 5 min before casting in a Teflon coated mould having the shape of a contact lens. After that the solution was allowed to undergo gel formation. It was observed that the solution turned into gel in 25 min. To confirm the formation of the hydrogel, the same experiment was carried out inside a vial and the formation of the hydrogel was confirmed through the vial inversion method. The as prepared hydrogel was dipped into an ethanol water mixture (1 : 4 volume ratio) for 24 h to get rid of the residual reactants from the hydrogel. After that the hydrogel was allowed to dry in a vacuum oven at 30 °C. It was observed that when the solution was cast at a thickness of <2 mm, it was not turbid. But more than 2 mm thickness resulted in a turbid hydrogel. At a thickness of 1.5 mm, the hydrogel provides a transmittance of 83% (Fig. S1a, ESI†), monitored using UV-vis spectroscopy. The restriction of the path of the light at higher thickness of the hydrogel due to the presence of more micro-phase separation in the thick hydrogel as compared to the thin hydrogel might be the reason behind the loss in transparency.[35,36] The presence of the hydrophobic PDMS segment and the hydrophilic poly(amine) (AmPGMA) segment creates the micro-phase separation.

The same process for hydrogel preparation was applied in the case of the zwitterionic polymersome incorporated hydrogel. Along with the amphiphilicity due to the presence of PDMS and AmPGMA segments, formation of the strong zwitterionic interactions in the presence of polyzwitterionic polymersomes also affects the transparency at higher thickness of the hydrogel. At high thickness, there is a chance of the formation of more zwitterionic interactions between the zwitterionic polymersomes, which can affect the transparency of the polymer film.[37] In our previous report, we have proved the formation of the crystalline domain by the polyzwitterionic segment *via* SAXS analysis.[28] In this case we observed 79% (Fig. S1b, ESI†) transmittance at a thickness of 1.5 mm. To prepare the curcumin loaded hydrogel, a curcumin drug loaded polyzwitterionic polymersome solution at a concentration of 20 mg ml^{-1} was thoroughly mixed with 10 ml of an aqueous solution of (concentration 300 mg ml^{-1}) AmPGMA-*b*-PDMS-*b*-AmPGMA BCP followed by the addition of 5 ml of polyethylene glycol-dialdehyde (concentration 100 mg ml^{-1}). The whole system was allowed to homogenize for 5 min and then cast over the mould. It was observed that the whole system turned into a gel after 18 min of standing. The vial inversion method was also applied in this case to confirm the formation of the hydrogel. In this case, 74% transmittance (Fig. S1c, ESI†) was observed for the curcumin loaded film with a thickness of 1.5 mm. It was observed that at higher thickness (2.5 mm), the transparency further reduced to 56% (Fig. S1d, ESI†). A PDMS based hydrogel having no curcumin was prepared as a control sample for the antimicrobial activity. Since the curcumin molecule can exist in keto/enol tautomeric form, it forms H-bonds between the amine groups of the amine functionalized PDMS BCP. This restricts the gel formation in the next step *via* a Schiff-base reaction between the aldehyde group of CHO–PEG–CHO and amine group of the amine functionalized PDMS BCP. As a result, a hydrogel was not formed. For this reason, we have encapsulated the curcumin drug in the zwitterionic polymersomes and dispersed accordingly during the hydrogelation.

2.2.7. Swelling study of the synthesized hydrogel. The swelling ratio of the synthesized PDMS based hydrogel was determined using the gravimetric method. To study the swelling of the hydrogel, a predetermined amount (400 mg) of the disc shaped hydrogel was dipped into PBS buffer solution having a pH of 7.4. After a definite time interval, the swollen hydrogel was taken out from the PBS buffer and the weight of the swollen hydrogel was taken after gently pressing the hydrogel with tissue paper to remove the excess surface buffer solution. The swelling ratio of the hydrogel was determined using the formula mentioned below

$$Q = \frac{W_{\text{Swollen}} - W_{\text{Dry}}}{W_{\text{Dry}}}$$

where W_{Dry} and W_{Swollen} are the dry and swollen weight of the hydrogel sample respectively.

2.2.8. Self-healing test. The self-healing property of the hydrogel was monitored using the ''scratch & heal'' method. To carry out the experiment, a micro notch was created over the hydrogel surface using an insulin syringe in its dried condition. After that, 1 ml of saline water (0.154 M) was added over the notched surface of the hydrogel and kept for 15 min. The self-healing efficiency of the hydrogel was monitored using optical microscopy, AFM, tensile tests and rheology analysis. The tensile test of the self-healed hydrogel was carried out to have an idea of the retention of the mechanical properties by the hydrogel after being cracked. For the self-healing experiment,

a hydrogel without the polyzwitterionic polymersome was taken as a control.

2.2.9. Mechanical properties. The tensile strength and elongation at break of the wet hydrogels (dimensions = 50 mm × 15 mm × 1.5 mm) were measured using a Hounsfield H10KS tensile test machine. Tensile test analysis was carried out to confirm the self-healing ability of the hydrogel. It was carried out by maintaining a crosshead speed of 10 mm min^{-1} using a load cell of 500 N at room temperature. All the hydrogel samples were brushed with silicone oil to prevent the evaporation of water from the hydrogel surface.

The isothermal rheology analysis of the PDMS based hydrogel in its swollen state was carried out using an Anton Paar (USA) parallel plate rheometer. In this case, the shear strain was varied from 0.001 to 10%, maintaining a constant angular frequency of 1 Hz at a 25 °C temperature. For the self-healing study, a cylindrical shaped hydrogel having a thickness of 0.3 cm was placed in a parallel plate rheometer. The shear strain was varied as mentioned earlier. The variation of the viscoelastic behavior of the synthesized PDMS based hydrogel samples was examined.

2.2.10. Protein adsorption assay. To study the antifouling activity of the synthesized hydrogel, a piece of square shaped hydrogel having a dimension of 1 × 1 cm^2 was dipped into 10 ml of 0.154 M BSA (concentration = 2 mg ml^{-1}) and left for 24 h at 37 °C. After the completion of the experiment, 3 ml of the BSA solution was withdrawn and the absorbance of the solution was measured using a UV-visible spectrophotometer at a maximum wavelength of 286 nm. To have an idea about the morphological change of the hydrogel surface after being treated with the BSA solution, FESEM analysis of the hydrogel surface was carried out. Before the analysis, the hydrogel sample was washed with excess PBS buffer solution (50 ml), so that the free BSA proteins over the hydrogel surface can be washed out. The protein adhesion study was carried out over both the hydrogel having the poly(zwitterionic) polymersome (experimental sample) and that without (w/o) the poly-(zwiterionic) polymersome (control sample).

2.2.11. Drug loading and *in vitro* release study. To encapsulate curcumin drug in the tri-block copolymer based polymersome, a predetermined amount of poly(zwitterionic) BCP (200 mg) was dissolved separately in DMF (5 ml) at a concentration of 40 mg ml^{-1} and then in the same solution curcumin drug was dissolved at a concentration of 2 mg ml^{-1}. The mixture was stirred for 10 min till complete homogenization. Then 20 ml PBS buffer of pH 7.4 was added dropwise to the resultant solution with subsequent stirring for 2 h to produce curcumin loaded polymersomes followed by dialysis of the resultant drug loaded polymersome solution using dialysis tube having a molecular weight cut off of 3 kDa. For the dialysis, the tube was immersed in 1 L of PBS buffer solution for complete removal of DMF. During the dialysis process, every 6 h the buffer solution was replaced with fresh buffer solution to ensure the complete removal of DMF. Then the polymersome solution was centrifuged at 5000 rpm for 10 min to settle out the unloaded curcumin. The amount of loaded curcumin was determined by using a UV-vis spectrophotometer with a standard calibration curve at a wavelength of 425 nm. The drug loading efficiency (DLE) and the drug loading content (DLC) were calculated by the following equations mentioned below

$$\mathrm{DLE}(\%) = \frac{(\text{Weight of loaded drug in nanoparticles})}{(\text{Weight of drug in feed})} \times 100$$

$$\mathrm{DLC}(\%) = \frac{(\text{Weight of loaded drug in nanoparticles})}{(\text{Total weight of the drug loaded nanoparticles})} \times 100$$

All the experiments were carried out in triplicate and the average data were presented.

After that, the curcumin loaded polymersome solution was freeze dried and was kept for further study. The procedure to prepare the drug loaded hydrogel has been explained previously.

To evaluate the curcumin release from the hydrogel sample, 200 mg of the gel was placed into 10 ml of PBS buffer solution (pH 7.4) enclosed in a dialysis bag having a molecular weight cut off of 3 KDa. After that the dialysis bag was transferred into an incubator shaker (60 rpm) and the temperature was maintained at 37 °C. During the incubation, the dialysis membrane filled with the hydrogel was dipped into 30 ml of PBS buffer kept in a closed conical flask. At predetermined time intervals, the PBS solution present outside the dialysis tube was taken out and centrifuged at 5000 rpm for 10 min to settle out the leached curcumin drug (as it is a hydrophobic drug) from the gel. Then the released curcumin was solubilized in 2 ml of ethanol and the amount of the released curcumin from the gel was determined using a UV-vis spectrophotometer at λ_{max} = 420 nm using a standard calibration curve of curcumin drug in ethanol. Here, we have used this method to protect the hydrogel sample from disintegration during continuous shaking. As we have studied the drug release study for more than 150 h, we believe that the hydrogel film will disintegrate in that time under shaking and can form small hydrogel particles. If we do not use the dialysis membrane as a barrier then the hydrogel particles formed during shaking can be separated out with the leached curcumin drug during centrifugation. This might interrupt the UV-vis analysis of the drug. The following equation was used to determine the amount of curcumin release:

$$\text{Curcumin release}\% = \frac{\text{Amount of the curcumin released at time } "t"}{\text{Total amount of the curcumin present in the hydrogel}} \times 100$$

2.2.12. Antimicrobial assay. An inhibition zone method was applied for the qualitative estimation of the antimicrobial activity provided by the curcumin incorporated encapsulated polymersome hydrogel. In a typical formulation for the preparation of a lysogeny broth (LB)-agar plate, tryptone (1 g), yeast extract (0.5 g), NaCl (1 g) and water (100 ml) were mixed thoroughly. The pH was adjusted to 7.0. After that, agar (2 g) was added to the solution and mixed well before autoclave sterilization. For this analysis, *Escherichia coli* (Gram-negative)

and *Staphylococcus aureus* (Gram-positive) were taken as model microbes. The bacterial samples were spread over the LB-agar plate individually using the pour plate technique before placing the hydrogel solution (in PBS of pH = 7.4) over it. A well method was adapted in this case to study the antimicrobial action by the hydrogels. After placing the sample over the agar plate, it was allowed to incubate for 24 h at 37 °C. The formed zone of inhibition was measured using the zone measurement scale. To study the repeatability of the experiments, the antimicrobial activity of the samples was observed three times and an average value has been reported in this manuscript.

2.2.13. Morphological analysis of bacteria. The morphological analysis of the drug treated bacteria was carried out *via* SEM analysis. To characterize the morphology of the bacteria after being treated with the curcumin loaded embedded polymersome hydrogel, log phase *S. aureus* and *E. coli* bacteria were cultured in fresh LB medium having the curcumin loaded polymersome containing hydrogel as a positive control and the zwitterionic hydrogel without curcumin encapsulation as a negative control. The whole solution was incubated for 3 h at 37 °C in a shaking incubator. Bacterial cells were collected *via* centrifugation and then washed thrice with PBS (pH 7.4) buffer. The isolated bacterial cells were then fixed with 2.5% glutaraldehyde solution for 2 h. After that the glass slide was washed with 50, 70, 85, 90, and 100% ethanol for 10 min to dehydrate the whole system. Before SEM imaging, all the samples were gold sputter-coated.

2.2.14. MTT colorimetry assay. The MTT colorimetric assay was carried out using the following mentioned protocol. For this study, human dermal fibroblast cells were harvested using trypsin–EDTA (Himedia, TCL144). After that, the cells were counted using a hemocytometer followed by seeding of the cells in a 96-well plate. The measured cell density was about 5000 cells per well. A high glucose DMEM medium (Gibco, 12800-017) with 10% FBS (Himedia, RM9955) was used to grow the cells. After 75% confluence growth of the cells, the media were altered to incomplete DMEM medium for treatment. The curcumin loaded hydrogel and the hydrogel devoid of curcumin were crushed and dispersed in PBS solution and sonicated to get a uniform solution. The dispersion was again mixed with incomplete DMEM medium. The final concentration of the dispersion was 50 μg ml^{-1}. Finally, the plates were incubated for 48 h, and the incomplete medium was replaced by 100 μl of MTT reagent (Thermo Fischer Scientific, M6494) per well (1 mg ml^{-1}). After the required incubation, a reading was taken at a wavelength of 550 nm using a microplate reader (Biorad) to determine the cytotoxicity.[38]

For the cytotoxicity of HaCat cells, a similar procedure was adopted to that explained above.

2.2.15. Statistical analysis. The protein adhesion assay and the antimicrobial assay were carried out in triplicate and the average values of all triplicate values (±standard deviation) were reported. Student's *t*-test was used to compare the statistical significance of the test samples against the control.

The characterization techniques have been explained in the ESI.†

3. Results and discussion

In this work, a tri-block copolymer based on PDMS was prepared *via* the RAFT polymerization method. A PDMS based macro-RAFT reagent was synthesized *via* modification of dihydroxy terminated PDMS (OH–PDMS–OH) using bromination followed by a xanthation reaction (Scheme S1, ESI†). After that this macro-RAFT reagent was used to prepare a zwitterionic tri-block copolymer

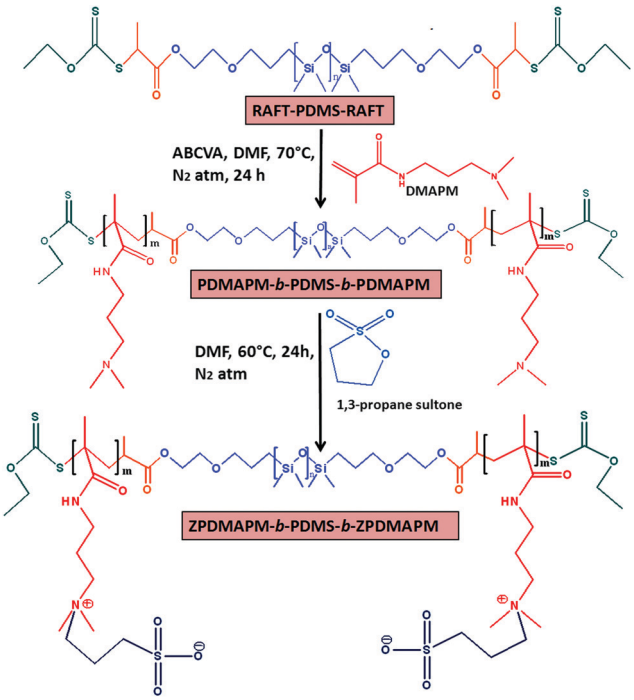

Scheme 1 Preparation of the zwitterionic modified PDMS tri-block copolymer.

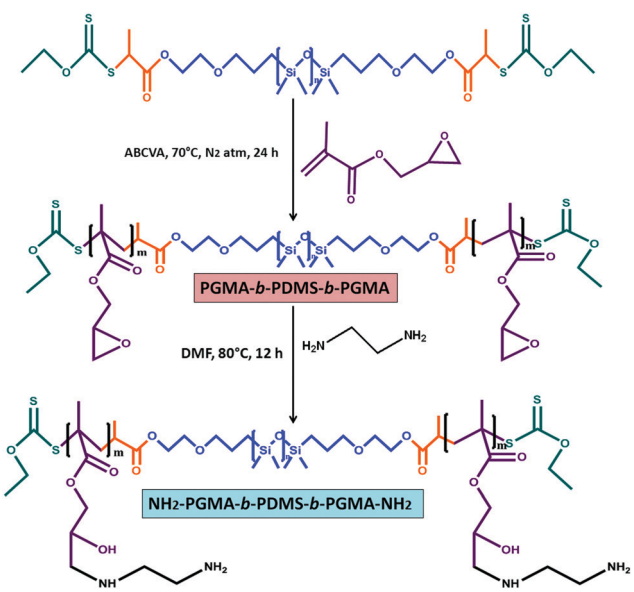

Scheme 2 Preparation of amine functionalized PDMS.

and amine modified PDMS block copolymers (Schemes 1 and 2). ^{1}H NMR analysis was utilized to elucidate the chemical structure of the modified PDMS and formed block copolymer. The ^{1}H NMR spectra of the pristine PDMS and bromine terminated PDMS are shown in Fig. S2 and S3 (ESI†) respectively and explained in the Experimental section. After xanthation of the brominated PDMS analogous new characteristic resonances appeared at δ = 4.66 ppm (i, CS-O-C**H**$_2$–) (Fig. 1a).

Using the PDMS-macro RAFT reagent, an ABA tri-block copolymer (PDMAPM$_{73}$-*b*-PDMS$_{65}$-*b*-PDMAPM$_{73}$) was synthesized using DMF as a solvent. The formation of the tri-block copolymer was confirmed by ^{1}H NMR analysis. The characteristic peaks for the second block (PDMAPM) appeared at δ = 2.29–2.33 ppm [o, –N-(C**H**$_3$)$_2$ and p, (CH$_3$)$_2$-N-C**H**$_2$–] and δ = 3.20 ppm (m, –CO-NH-C**H**$_2$–) (Fig. 1b). The molecular weight of the tri-block copolymer was calculated to be $M_{n/GPC}$ = 30 500 g mol^{-1}, having a $Đ$ of 1.34 (Fig. S4, ESI†). Upon betainization, several new peaks appeared at δ = 2.94 ppm (**s**, –C**H**$_3$-SO$_3^-$), δ = 3.10 ppm (**p**, [–N(CH$_2$)(C**H**$_3$)$_2$]$^+$) and δ = 3.46 ppm (q, [–N(C**H**$_2$)(CH$_3$)$_2$]$^+$).

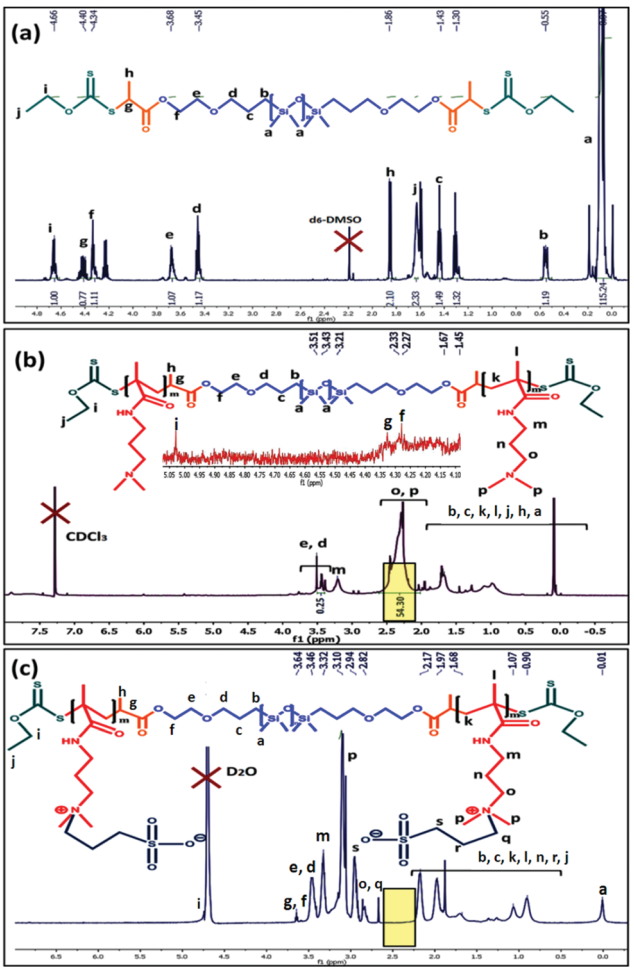

Fig. 1 ^{1}H NMR analysis of the (a) PDMS-xanthate macro RAFT reagent; (b) PDMAPM-*b*-PDMS-*b*-PDMAPM tri-block copolymer and (c) PDMS based zwitterionic tri-block copolymer (ZPDMAPM-*b*-PDMS-*b*-ZPDMAPM).

The shifting of the peak from δ = 2.29 ppm (–N-(C**H**$_3$)$_2$) to δ = 3.10 ppm ([–N(CH$_2$)(C**H**$_3$)$_2$]$^+$) (Fig. 1c) indicates the successful betainization (approximately 100% determined from NMR analysis, indicated with the yellow highlight in Fig. 1) of the tertiary amine to form the polyzwitterionic tri-block copolymer (z-BCP).

To prepare the amine functionalized PDMS BCP, initially the PDMS-macro RAFT reagent was utilized to prepare a PGMA incorporated tri-block copolymer (PGMA$_{93}$-*b*-PDMS$_{65}$-*b*-PGMA$_{93}$) followed by amination with EDA (Scheme 2). Characteristic peaks for the PGMA segment appeared at δ = 2.65 ppm and 2.86 ppm (**o**, –C**H**$_2$-O-CH–), δ = 3.25 ppm (**n**, –CH$_2$-O-C**H**–) and at δ = 3.84 ppm and 4.31 ppm (**m**, –COO-C**H**$_2$–) (Fig. 2a). For the tri-block copolymer, a number average molecular weight (M_n) of 32 000 g mol^{-1} was observed from GPC analysis, having a $Đ$ of 1.42 (Fig. S4, ESI†). The obtained value of $Đ$ designates the successful control radical polymerization between the PDMS-macro RAFT reagent and GMA.[39]

Upon amination of the PGMA unit, new characteristics peaks appeared at δ = 2.79 ppm (**p**, –NH-C**H**$_2$-C**H**$_2$-NH$_2$), δ = 2.91 ppm (**o**, –CH-C**H**$_2$-NH–) and at δ = 3.13 ppm (**n**, –C**H**-OH) (Fig. 2b).

The bifunctional crosslinker poly(ethyleneglycol) dialdehyde (Ald-PEG-Ald) was prepared and characterized using ^{1}H NMR analysis as explained in the Experimental section (Fig. S5, ESI†).

The formation of the copolymer (PDMAPM-*b*-PDMS-*b*-PDMAPM) was further characterized with FTIR analysis. Pristine PDMS showed characteristic absorption peaks at 1033 cm^{-1} and 1192 cm^{-1} for Si–O–Si stretching, 1265 cm^{-1} due to CH$_3$ symmetric bending in Si-CH$_3$, 2975 cm^{-1} for C–H stretching in CH$_3$ and 3412 cm^{-1} due to OH$^-$ stretching.[40] After the formation

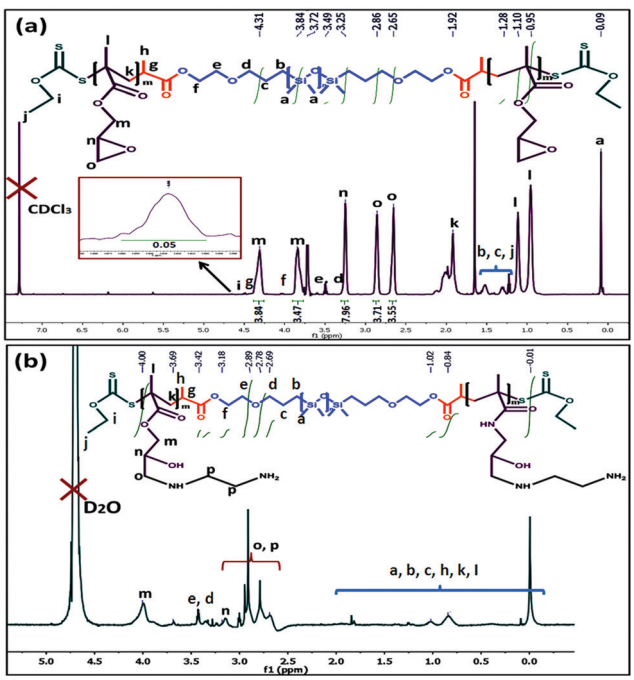

Fig. 2 ^{1}H NMR analysis of the (a) PGMA-*b*-PDMS-*b*-PGMA tri-block copolymer and (b) amine modified PDMS based tri-block copolymer (AmPGMA-*b*-PDMS-*b*-AmPGMA).

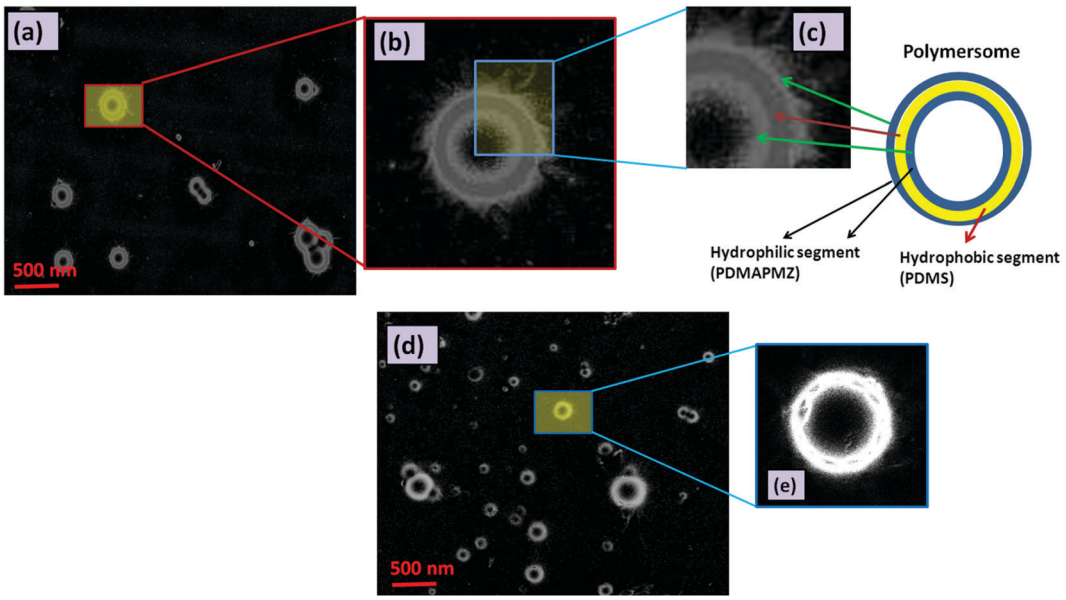

Fig. 3 HRTEM image of the (a) ZPDMAPM-*b*-PDMS-*b*-ZPDMAPM tri-block copolymer based polymersome; (b) and (c) magnified view of the polyzwitterionic polymersome; (d) amine modified PDMS tri-block copolymer (AmPGMA-*b*-PDMS-*b*-AmPGMA) based polymersome and (e) magnified view of the amine functionalized polymersome.

of the block co-polymer (PDMAPM-*b*-PDMS-*b*-PDMAPM), new absorption bands appeared at 1431 cm^{-1}, 1732 cm^{-1} and 2930–2840 cm^{-1} due to the presence of C–N stretching, >C=O group stretching and asymmetric and symmetric stretching of the $-CH_2$ group, respectively. After the treatment with 1,3-propane sultone, characteristic absorption bands appeared at 931 cm^{-1} and 1477 cm^{-1} ($-CH_3$ stretching and bending vibrations of $[RN(CH_3)_3]^+$), and 1033 cm^{-1} and 1193 cm^{-1} (symmetric and antisymmetric vibrational peaks of the SO_3^- group), indicating the betainization of the PDMAPM group (Fig. S6, ESI†).[41]

FTIR analysis was also utilized to find out the functionality present in the PGMA-*b*-PDMS-*b*-PGMA tri-block copolymer. Due to the presence of the PGMA segment, characteristic absorption bands appeared at 850 cm^{-1} and 915 cm^{-1} (oxirane ring

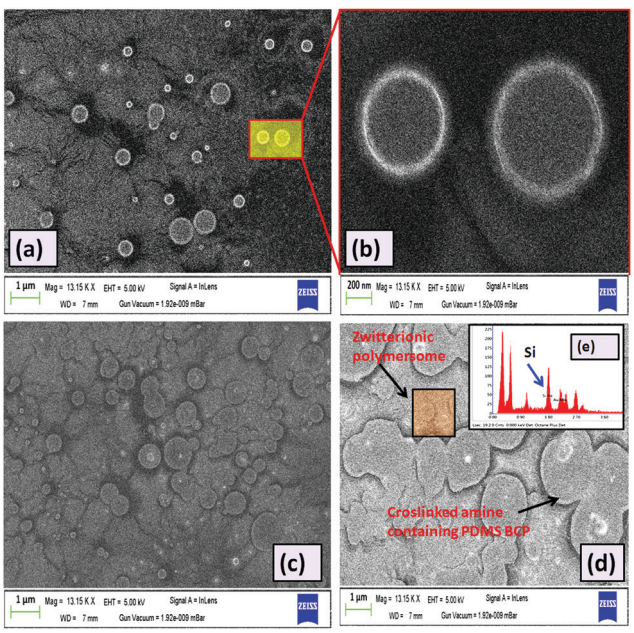

Fig. 4 FESEM images of the (a) ZPDMAPM-*b*-PDMS-*b*-ZPDMAPM tri-block copolymer based polymersome; (b) magnified view of the polymersome; (c) amine modified PDMS tri-block copolymer (AmPGMA-*b*-PDMS-*b*-AmPGMA) based polymersome; and (d) curcumin loaded polyzwitterionic polymersome incorporated PDMS-NH_2 crosslinked hydrogel and (e) elemental analysis of the hydrogel.

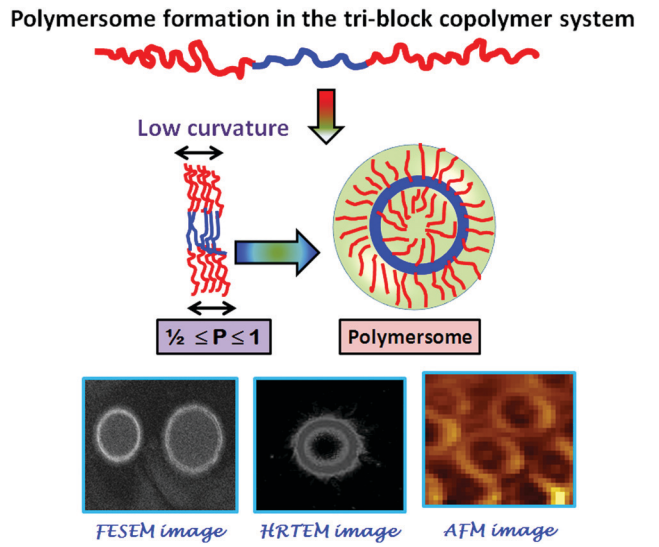

Scheme 3 Schematic representation of the probable mechanism of self-assembly by the synthesized tri-block copolymers.

asymmetric contraction and expansion), 1135 cm^{-1} (C–O–C stretching vibration) and 1736 cm^{-1} (stretching of the >C=O group).[42] Upon modification with ethylene diamine (EDA), the absorption bands at 850 cm^{-1} and 915 cm^{-1} disappeared. This indicates the successful ring opening by the EDA segment. A bunch of new peaks appeared at 1495 cm^{-1} (C–N stretching), 1582 cm^{-1} (N–H stretching) and 3445 cm^{-1} (O–H stretching) due to the presence of the EDA addition (Fig. S7, ESI†).[43]

3.1. Self-assembly behavior of the tri-block copolymer in aqueous solution and study of its morphology

Amphiphilic BCPs having ionic segments as one of the blocks are an interesting class of macromolecules due to their fascinating range of self-assembled structures including spherical, lamellar, rod-like, vesicular *etc.*[44] Among different morphological orientations of BCPs, the vesicular structure is an important class of

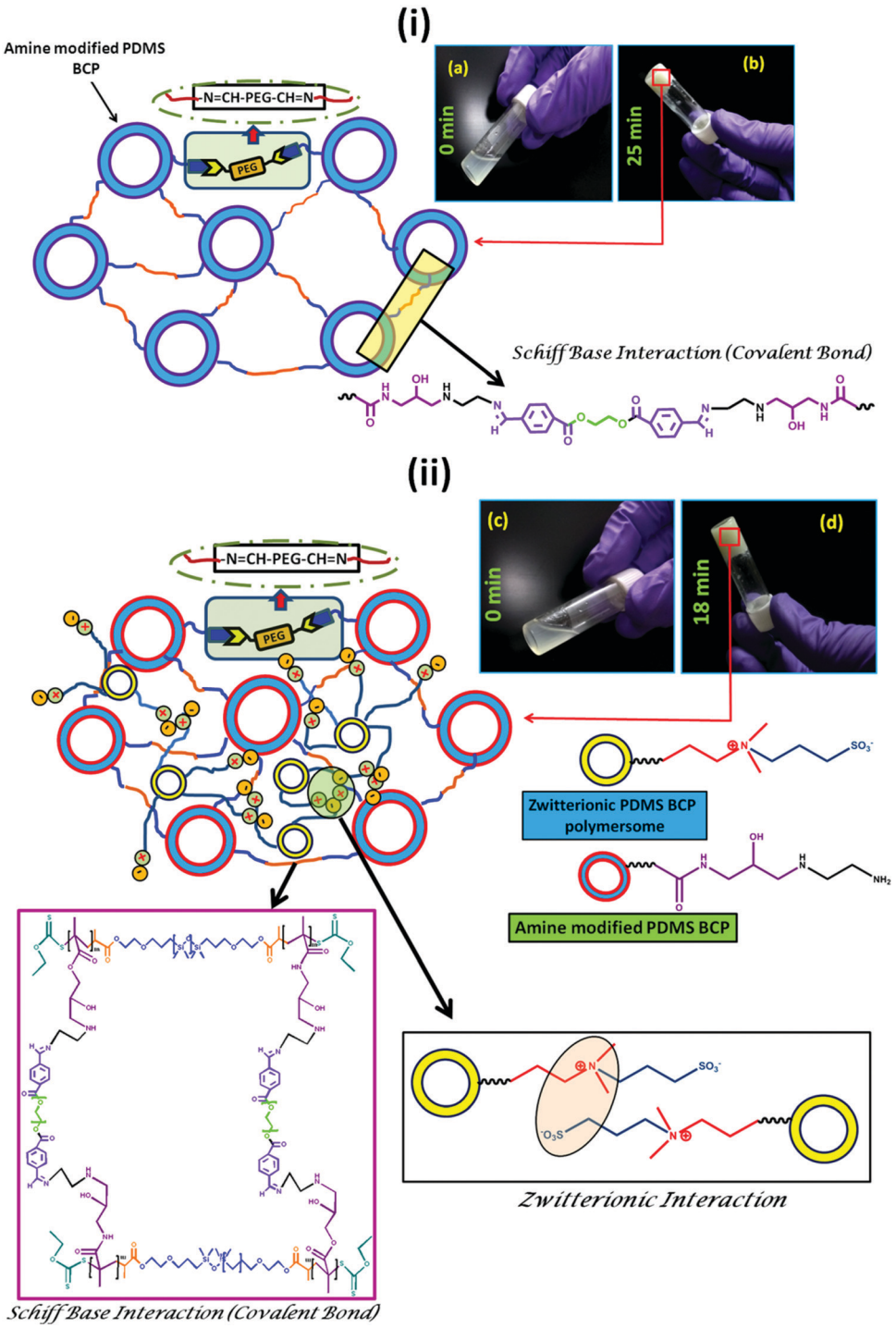

Scheme 4 Synthesis scheme of the PDMS based hydrogel (i) without and (ii) with the polyzwitterionic polymersome.

self-assembled structures of polymers because of its resemblance to liposomes (lipid vesicles). In our study, we have monitored the self-assembly of BCPs *via* HRTEM, FESEM and AFM analyses.

Fig. 3a shows the polymersome formed by ZPDMAPM-*b*-PDMS-*b*-ZPDMAPM. This polymersome has three distinct layers as evidenced by HRTEM images. The enlarged images of the distribution of the tri layer have been shown in Fig. 3b and c. AmPGMA-*b*-PDMS-*b*-AmPGMA also shows a similar type of morphology (Fig. 3d) (enlarged image shown in Fig. 3e). The DLS analysis showed that the polyzwitterionic polymersomes have a particle size of 265 ± 5 nm with a particle distribution index (PDI) of 0.352 (Fig. S8a, ESI†). A high value of the PDI indicates ionic interactions between the polyzwitterionic segments. The curcumin loaded zwiterionic polymersomes have a bit bigger particle size of 282 ± 4 nm with a PDI of 0.379 (Fig. S8b, ESI†). Whereas, the amine modified PDMS polymersomes have a particle size of 255 ± 5 nm with a PDI of 0.334. The zeta potential of the zwitterionic polymersomes was also measured and it was 1.44 mV.

Like the HRTEM images, FESEM analysis also indicates a ring like morphology (polymersome) for the PDMS based tri-block copolymers in the presence of water. Both ZPDMAPM-*b*-PDMS-*b*-ZPDMAPM (Fig. 4a) [Fig. 4b is the zoomed image of the zwitterionic polymersome] and AmPGMA-*b*-PDMS-*b*-AmPGMA (Fig. 4c) acquired a ring like morphology in the presence of water. The interaction of the polyzwitterionic polymersomes inside the bulk of the PDMS based hydrogel was evidenced by FESEM analysis as shown in Fig. 4d. The elemental mapping of the self-assembled BCP has revealed the presence of silicon (Si), confirming the existence of PDMS in the self-assembled structure (Fig. 4e). The FESEM images of the PDMS-NH_2 polymersome crosslinked hydrogel and polyzwitterionic polymersome incorporated PDMS-NH_2 crosslinked hydrogel have been shown in Fig. S9 (ESI†).

Formation of this type of polymersome morphology is governed by several factors like the nature of the solvent, the block length ratio of the segments present in the BCP and the polymer–solvent interaction parameter (χ), which is directly related to the solubility parameter (δ) and the dielectric constant value of the solvent (ε).

In water, the hydrophobic segment of the BCP (like PDMS) tries to orient itself so that it has minimum interaction with the water. The self-assembly offered by BCPs is mainly due to the unfavorable mixing enthalpy, which allows the micro-phase separation in the BCP.

The difference in the solubility of the different segments of BCP has an important effect over the formation of the curved structure rather remains as a flat layered sheet form. Formation of a thermodynamic instability gradient by the different blocks of the BCP provokes the system to be curved and adopt the vesicular morphology. By accepting the curved morphology, the free energy of the hydrophilic layer gets increased while the reverse thermodynamic phenomenon occurs for the hydrophobic segments. The obtained AFM images (Fig. S10, ESI†) also corroborate the results obtained in the HRTEM and FESEM analyses. Fig. S10 (ESI†) shows that the soft segment PDMS (dark brown color) occupies the middle layer of the tri-block copolymer, whereas the hard polyzwitterionic segment (bright yellow color) finds the terminal part of the tri-block copolymer. It is reported that the interfacial curvature of the lamellar structure is related to the packing parameter (P), which can be expressed as follows:

$$P = \frac{V_c}{L_c A_c} = 1 - HL_c + \frac{K_G L_c^2}{3}$$

where P = packing parameter; A_c = the interfacial area between the hydrophilic and hydrophobic segments; V_c and L_c are the volume and length of the hydrophobic segments of the amphiphilic BCP, H = mean curvature and K_G = Gaussian curvature.

The geometry and the molecular shape of the self-assembly depend on the packing parameter value (P). It is reported that if the "P" value for a tri-block copolymer is in the range of $1/2 \leq P \leq 1$, it will orient itself in a polymersome shape like in our present system.[45] The mechanism of the formation of the polymersome has been schematically represented in Scheme 3.

3.2. Preparation and properties of the hydrogel

The hydrogel was prepared using Schiff-base chemistry. As the Schiff-base reaction between an amino and an aldehyde group to form an imine linkage can be carried out at physiological pH,

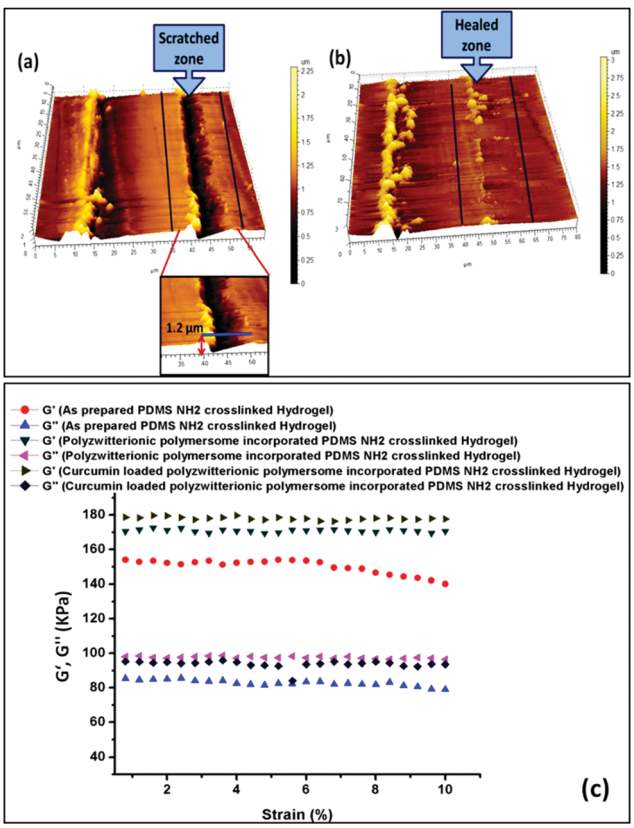

Fig. 5 Study of the self-healing activity through AFM depth profilometry, carried out in tapping mode: (a) 3D image of the cut and (b) 3D image of the self-healed zone and (c) rheology analysis of the synthesized PDMS based hydrogels.

it increases its biocompatibility. The amine modified PDMS based tri-block copolymer was crosslinked with dialdehyde modified poly(ethylene glycol) (Ald-PEG-Ald). Rapid formation of crosslinking *via* formation of imine bonds was observed when the amine modified PDMS solution comes into contact with the aqueous solution of the aldehyde modified PEG. The formation of the imine bonds and subsequent gelation was very rapid (25 min) and was confirmed through the inversion vial method (Scheme 4(i)a and (i)b). It was observed that in the presence of polyzwitterionic polymersomes the gelation time reduced significantly to 18 min. In this case also the formation of the hydrogel was confirmed through the inverse vial method (Scheme 4(ii)c and (ii)d). The probable reason behind the rapid gelation may be due to the formation of zwitterionic interlocking along with the formation of imine bonds.[28,46,47]

The change in the hydrophilicity of the PDMS based hydrogel with incorporation of the polyzwitterionic polymersome and curcumin loaded polyzwitterionic polymersomes was evaluated by water contact angle (WCA) analysis. It was observed that the WCA value for the pure PDMS based hydrogel ($\theta_c = 110^\circ$) altered in the presence of polyzwitterionic polymersome incorporation and it reduced to $\theta_c = 94^\circ$. Upon incorporation of the hydrophobic drug loaded polymersomes into the PDMS based hydrogel formulations, a significant increase in the water contact angle ($\theta_c = 102^\circ$) value was observed. It can be explained by considering the fact that the curcumin drug loaded polymersomes occupied the free space of the network structure in the bulk of the PDMS hydrogel, which directly imparts hydrophobicity to the surface (Fig. S11a, ESI†).

The swelling of the formed hydrogel was measured through the gravimetric method. As explained in the experimental section a predetermined amount of a disc shaped hydrogel was dipped into water and the swelling of the hydrogel measured through a relative water uptake study. It was observed that the PDMS based hydrogel showed lower swellability ($Q_e = 12\%$) as compared to the hydrogel having the polyzwitterionic polymersome ($Q_e = 20\%$) (Fig. S11b, ESI†). Upon loading of the hydrophobic drug curcumin, the % swelling value again comes down to 16% (Q_e).

Differential scanning calorimetry (DSC) analysis was carried out to get an idea about the thermal response given by the

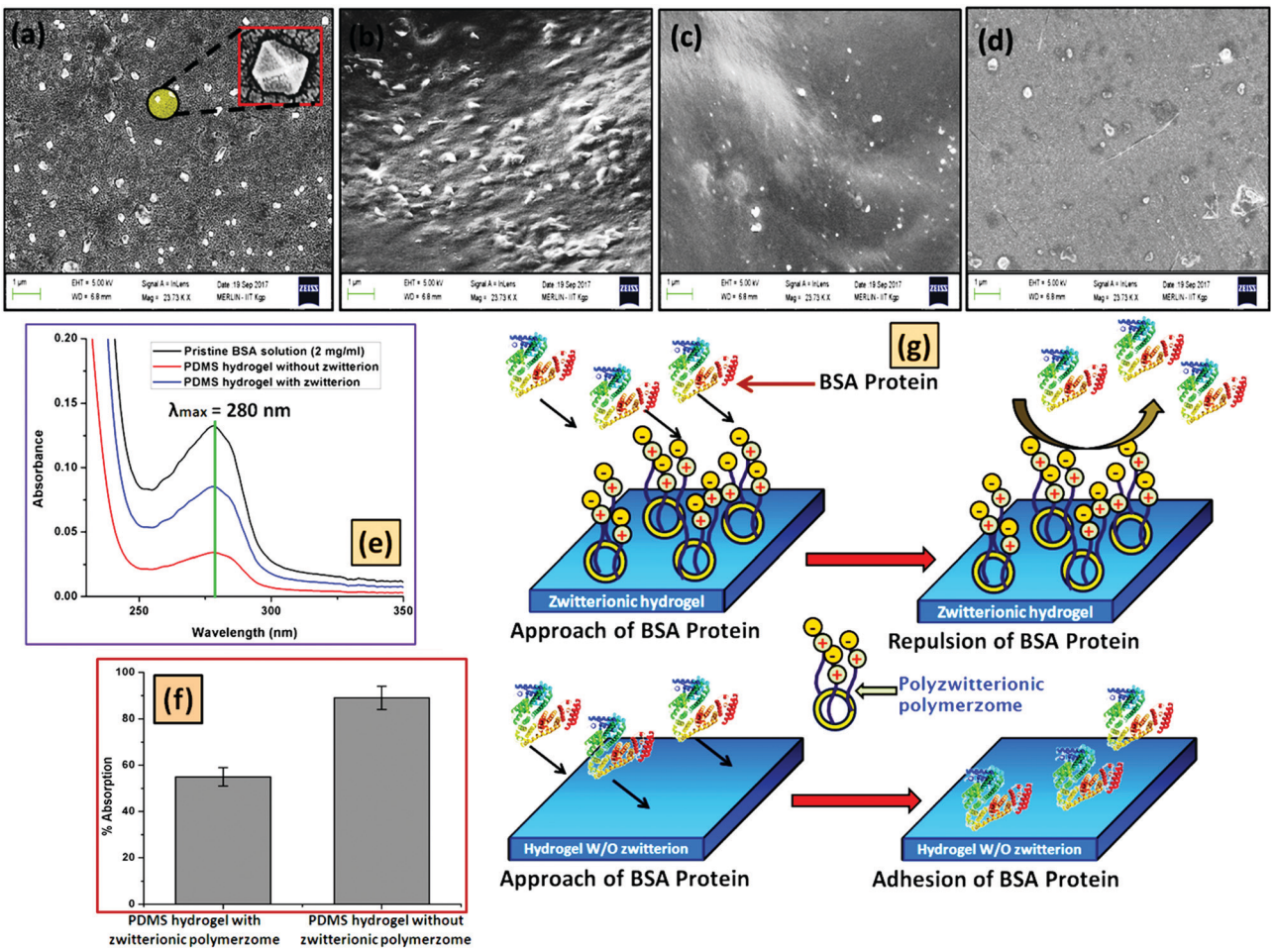

Fig. 6 FESEM images of (a) BSA protein cast over the glass slide; (b) BSA protein adsorbed over the PDMS based hydrogel without (w/o) entrapped polyzwitterionic polymersome; BSA protein adsorbed over the PDMS based hydrogel having entrapped polyzwitterionic polymersome at (c) the initial day of study and (d) after 7 days of dipping into BSA solution; (e) analysis of the BSA adsorption through UV-vis analysis; (f) protein adsorption (%) over the hydrogel surface calculated using the calibration curve and (g) schematic of the antifouling activity of the hydrogel.

zwitterionic PDMS based hydrogel system. From the DSC analysis (Fig. S12, ESI†), it was observed that the hydrogel is stable up to 250 °C with no strong deviation in the DSC traces.

3.3. Study of self-healing and mechanical properties

We have adopted a "scratch and heal" method in the case of our synthesized hydrogel to have an idea about its self-healing ability. In this case, we created a notch over the hydrogel (zwitterionic polymersome incorporated PDMS hydrogel) surface using an insulin syringe and then the notched hydrogel was treated with saline solution (0.154 M NaCl solution). It was kept for 20 min before the optical microscope imaging of the scratched and healed surface. The as prepared PDMS based hydrogel having no zwitterionic polymersomes was taken as a control. It was observed that in the case of the zwitterionic polymersome incorporated hydrogel, rapid and significant healing occurred repeatedly, whereas for the pure PDMS hydrogel the cut remained the same after the salt solution treatment (Fig. S13, ESI†). The self-healing in the case of the zwitteionic polymersome incorporated hydrogel was the effect of the reformation of the ionic bonds after the application of the saline solution which were ruptured during the cut. After the application of saline water, the hydrogel surface swelled up and the ionic counterparts of the polyzwitterionic segments came closer to each other and reformation of the ionic bonds occurred *via* the participation of the quaternary ammonium cations ($-N(CH_3)_3^+$) and the sulfonate anions ($-SO_3^-$).[26] The healing in the hydrogel system was also analyzed through AFM analysis and Fig. 5 presents the obtained results. The 3D image of the cut (Fig. 5a) and the healed (Fig. 5b) surface obtained from AFM analysis delineates the successful healing of the surface.

It is reported that silicone based hydrogels are relatively stiffer than conventional PHEMA based hydrogels due to the presence of silicone.[48] In our study we have found that the as prepared PDMS based hydrogel has a modulus of 0.15 (MPa), having an elongation before break (EB%) of 155%. After the incorporation of the curcumin loaded polyzwitterionic polymersome in the recipe of the PDMS hydrogel preparation, an increase in the modulus value (0.18 MPa) and a significant increase in the EB% (340%) were observed. The high percentage of elongation in the case of the polymersome incorporated PDMS hydrogel can be explained *via* considering the formation of the ionic interlocking between the zwitterionic segments. A significant elongation of ~340% of the hydrogel was observed before break, because of the presence of elastic ionic interactions. As a consequence, the toughness of the hydrogel was higher as compared to the normal PDMS hydrogel (control). The mechanical properties of the self-healed hydrogel were also monitored to have an idea about the retention of the mechanical properties after minor structural failure. It was observed that the modulus of the self-healed hydrogel reduced to 0.16 MPa and also the % elongation before break reduced to some extent (270%) (Fig. S14, ESI†). Though the ionic bonds were reformed after the treatment with salt water, the disruption of covalent bonds which were formed due to the Schiff-base reaction can't be patched up at the mentioned time.

In much of the literature, it is reported that the healing due to a Schiff-base reaction takes more than 30 min in basic conditions (pH > 8). Whereas, in water induced healing, a Schiff-base based hydrogel takes more than 60 min to heal.[49,50] In our system, the healing is rapid (within 15 min) in the presence of PBS solution having pH 7.4. Due to the lack of reformation of the covalent bonds *via* the Schiff-base reaction, a reduction in the modulus and the EB% value was observed. In every case, the modulus values of the hydrogels are to some extent closer to the market available contact lenses like Acuvue® 2 (0.29 MPa) and Acuvue® TruEye® (0.66 MPa). The tensile value of all the synthesized hydrogels has been shown in Fig. S14 (ESI†).

Fig. 5c shows the isothermal (temp 25 °C) viscoelastic properties of the synthesized hydrogels where the strain % was varied from 0.001% to 10% at a constant frequency of 1 Hz. The rheology analysis was carried out in compression mode where G' and G'' depict the elastic and viscous response given by the hydrogel during the application of the shearing force. From Fig. 5c, it was observed that the curcumin loaded hydrogel showed a higher elastic modulus compared to the rest. Apart from this, the presence of the polyzwitterionic polymersomes imparts a significant elasticity to the hydrogel system. Interestingly, it was observed from the rheo curve that a drop in the elastic modulus (G') value occurred in the case of the PDMS based hydrogel devoid of zwitterionic polymersomes at 6% strain. This is not the scenario for the PDMS based hydrogel having dual crosslinking (Schiff-base mediated covalent crosslinking and zwitterionic crosslinking). A synergistic effect of covalent crosslinking due to

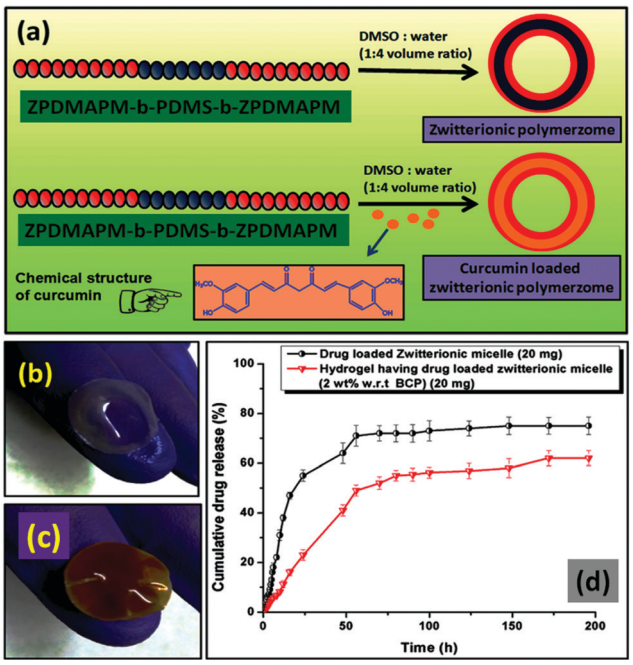

Fig. 7 (a) Schematic of the formation of the polymersome and the drug encapsulation; images of the prepared (b) pristine PDMS based hydrogel and (c) curcumin loaded hydrogel and (d) curcumin release study from the drug loaded polymersome and drug loaded entrapped polymersome hydrogel.

the Schiff-base reaction, zwitterionic interactions between the ionic polymersomes and hydrophobic–hydrophobic interactions between the curcumin drug molecules was the reason behind the elastic stability of the PDMS based hydrogel under variation of the strain %.

The self-healing property of the soft contact lens was further cross-checked *via* rheological analysis. From Fig. S15 (ESI†), it was observed that there was a deviation in the elastic (G') and the viscous modulus (G'') values in the self-healed sample compared to the same in the pristine hydrogel sample. As explained earlier in the tensile analysis, the decrease in the modulus value after the self-healing can be attributed to the elimination of the covalent bonds during scratch formation and only the formation of the ionic clusters between the quaternary ammonium cations ($-N(CH_3)^{3+}$) and the sulfonate anions ($-SO_3^-$) played a major role in retaining the modulus.

3.4. Protein adhesion assay

The extensive use of a soft contact lens by the patient enhances the chance of protein deposition. The reduction of the protein deposition over the contact lens surface is a challenging task. Due to the hydrophobicity of a pure silicon based hydrogel, it is very much prone to the deposition of proteins.[48,51] In this work, the antifouling activity of the prepared polyzwitterionic entrapped polymersome PDMS based hydrogel was evaluated by the adsorption of the BSA protein over the hydrogel surface. The respective calibration curve has been given in Fig. S16 (ESI†). The surface morphology of the protein treated hydrogel was observed through FESEM analysis (Fig. 6). The PDMS based hydrogel without the polyzwitterionic polymersome was taken as a positive control, whereas the polymersome containing hydrogel was taken as a negative control. Fig. 6a presents the morphology of the BSA protein. From the study, it was observed that the BSA protein was very much prone to adhere to the PDMS based hydrogel surface (Fig. 6b) but the scenario changed when the PDMS hydrogel has the polyzwitterionic polymersomes. The presence of the polyzwitterionic segments enhances the water adsorption capacity of the hydrogel, which results in a surface having antifouling activity. The presence of the thin layer of water over the hydrogel surface due to the presence of the polymersomes restricted the formation of biofilms (deposition of the BSA protein layer) (Fig. 6c). It is

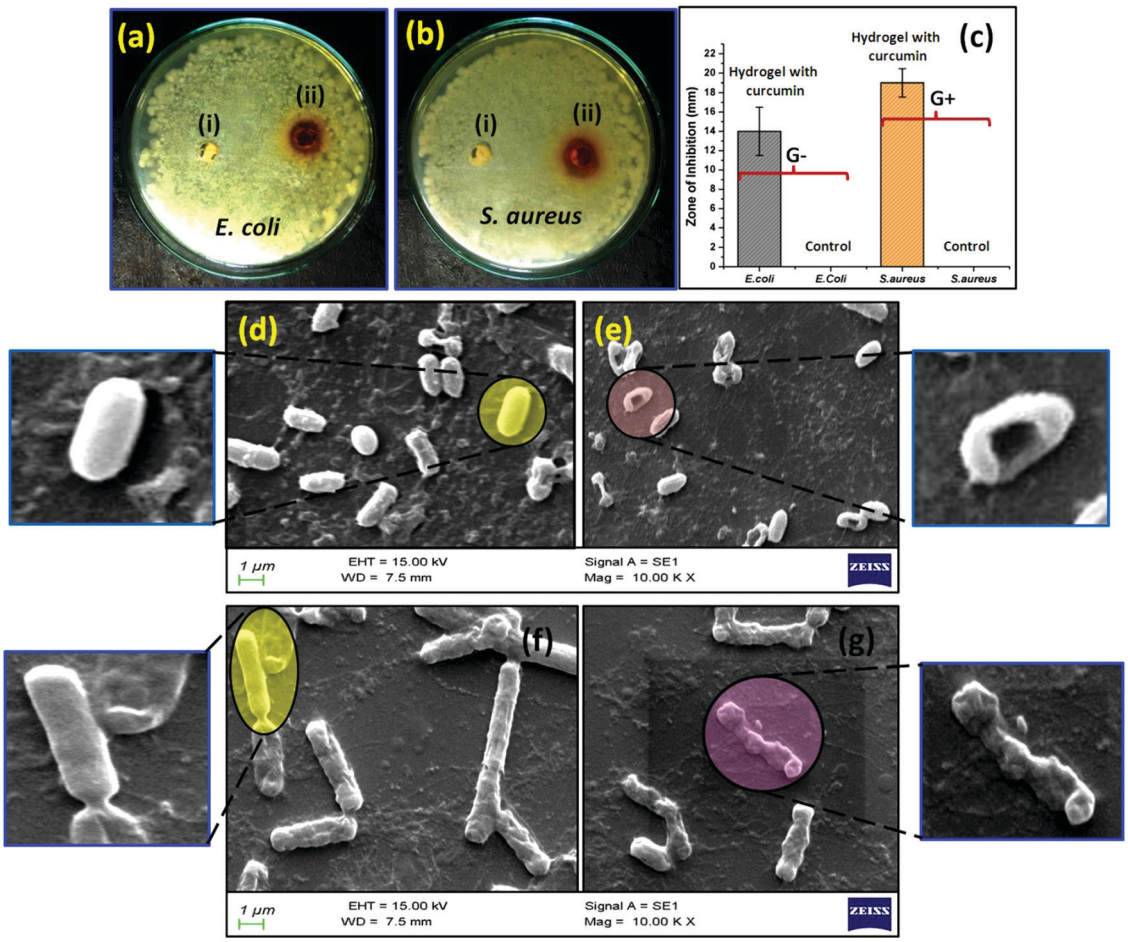

Fig. 8 Antimicrobial activity of the (i) pristine polyzwitterionic hydrogel and (ii) curcumin loaded polyzwitterionic hydrogel against (a) Gram negative *E. coli* and (b) Gram positive *S. aureus* bacteria; (c) summary of the obtained zone of inhibition values in graphical format. The morphological analysis of the (d) live and (e) dead *S. aureus* bacteria and (f) live and (g) dead *E. coli* bacteria through FESEM analysis.

reported that the polyzwitterionic segment conforms to an open chain structure in the presence of the salt solution due to its "anti-polyelectrolyte" behavior, which accelerates the antifouling activity.[52,53] Here, we have carried out the protein adhesion experiment in the presence of 0.154 M NaCl solution, which is the physiological salt solution concentration. As per the recent trends in contact lenses, most of the commercially available contact lenses can be used for a minimum of one day to a maximum of seven days depending on the quality of the soft contact lens. We have carried out the antifouling test over the hydrogel after dipping the hydrogel into a salt solution of BSA solution for 7 days and the FESEM image was captured (Fig. 6d). We have found a comparable antifouling property to the newly synthesized hydrogel film. Interestingly, it was observed that the presence of the polyzwitterionic polymersome drastically reduced the deposition of the protein, which was elucidated by UV-vis analysis (Fig. 6e). As described earlier, for the antifouling test, a hydrogel sample having dimensions of 1×1 cm^2 was dipped into a BSA solution of concentration 2 mg ml^{-1} for 24 h at 37 °C. After that, a predetermined amount of the BSA solution (1 mL) was withdrawn and the absorbance was measured at λ_{max} = 280 nm (characteristic absorbance value for the BSA protein). From the obtained absorbance value, it was observed that in the case of the polyzwitterionic PDMS hydrogel, the absorbance value was decreased drastically as compared to the PDMS hydrogel without (w/o) polymersomes. This supports the antifouling action of the polyzwitterionic hydrogel. The extent of the protein adsorption (Fig. 6f) over the surface was measured quantitatively through comparison of the obtained absorbance value with the calibration curve of BSA (Fig. S16, ESI†). The probable mechanism of the role of the hydrogel has been schematically represented in Fig. 6g.

3.5. Drug encapsulation, release and antimicrobial study

As discussed in the Experimental section, the zwitterionic BCP polymersome was loaded with curcumin drug during formation

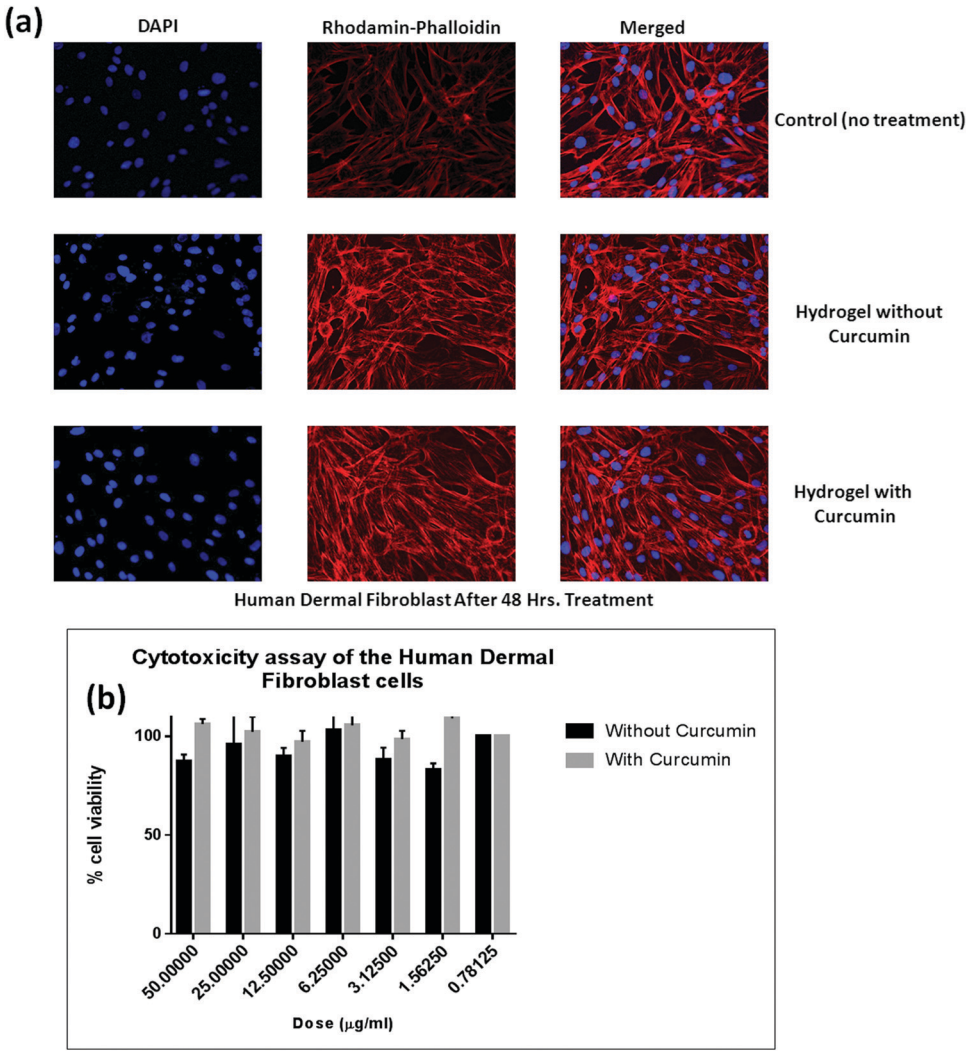

Fig. 9 (a) Confocal fluorescence microscopy image of the fibroblast cell line treated with the pristine hydrogel and the curcumin loaded hydrogel. The red panel denotes cytoskeletal staining by rhodamin–phalloidin and the blue panel denotes nuclear staining by DAPI. A merged panel is also given. (b) Respective % cell viability.

of the polymersomes to get an encapsulated curcumin zwitterionic polymersome.

A 4.2% drug loading capacity (DLC) and 63.4% drug loading efficiency (DLE) were observed for the zwitterionic polymersome. Due to the presence of the hydrophobic segment (PDMS), curcumin drug was entrapped in the core during the formation of the polymersome. After that the drug loaded polymersome was encapsulated in the PDMS based hydrogel. A schematic representation of the whole process is presented in Fig. 7a. The chemical structure of the curcumin drug has been shown in the inset of Fig. 7a. The images of the pristine PDMS hydrogel and the drug loaded PDMS hydrogel based contact lens have been showcased in Fig. 7(b) and (c) respectively. The curcumin drug release study was carried out at pH 7.4, the physiological pH of the human body. It was carried out for both the curcumin loaded zwitterionic polymersome and the drug loaded entrapped polymersome PDMS hydrogel (Fig. 7d). It was observed that in the case of the drug loaded polymersome, a burst release of the drug occurred, whereas the drug loaded polymersome containing hydrogel showed sustained delivery of the drug molecules. The reason behind the sustained release of the drug can be explained by considering the effect of the network structure of the hydrogel formed by the Schiff-base reaction between the amine modified PDMS and the aldehyde modified PEG. The network structure present in the bulk of the hydrogel creates a barrier to the curcumin drug and controls its release. This type of sustained release of the drug is very much crucial for long term use and can effectively reduce the multi-time intake of the drug, which is a problem in the case of applying eye drop solution.

The bactericidal activity of the synthesized hydrogel was measured through antimicrobial assay. The zone of inhibition formed as a result of the bactericidal activity of the hydrogel was monitored to quantify the antimicrobial effect of the formed hydrogels. The antimicrobial activity of the curcumin loaded hydrogel was tested against Gram negative bacteria *E. coli* (Fig. 8a) and Gram positive bacteria *S. aureus* (Fig. 8b). Here, the entrapped polymersome hydrogel having no curcumin content was taken as a positive control, whereas the curcumin

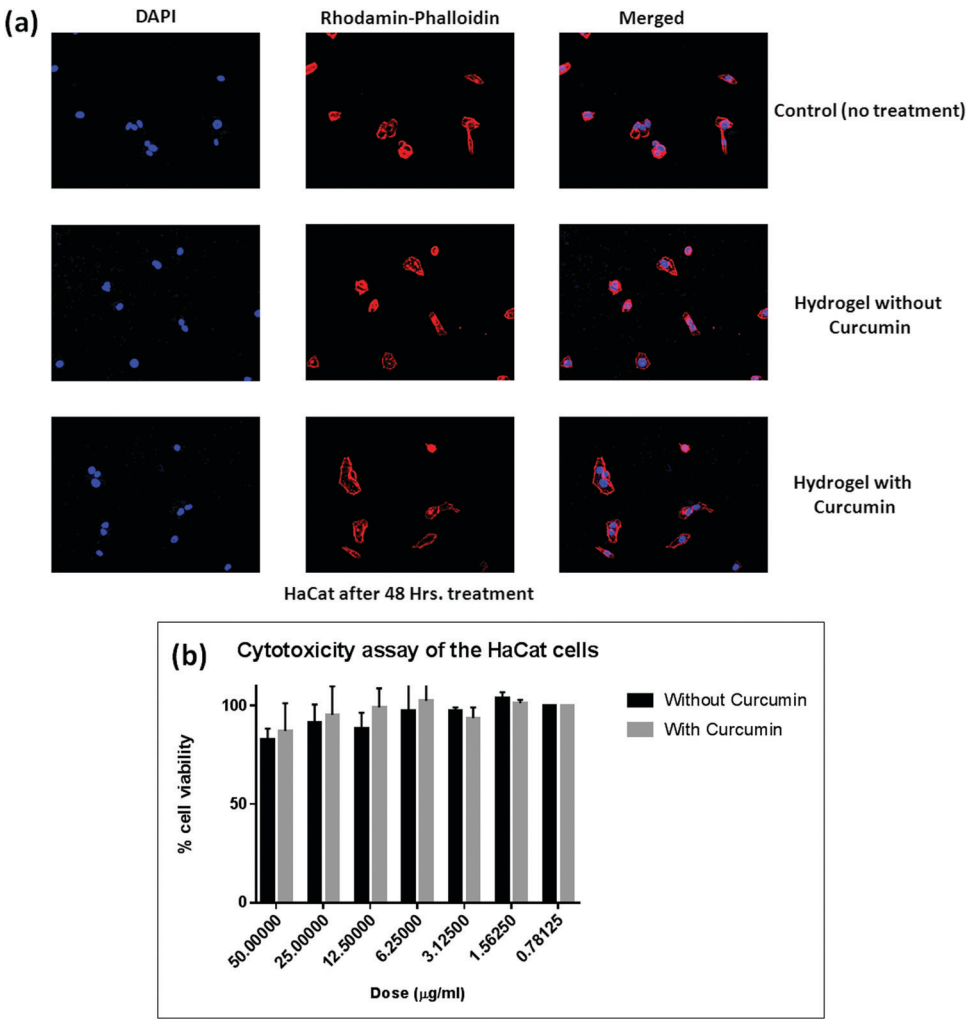

Fig. 10 (a) Confocal fluorescence microscopy image of the HaCat cell line treated with the pristine hydrogel and the curcumin loaded hydrogel. The red panel denotes cytoskeletal staining by rhodamin–phalloidin and the blue panel denotes nuclear staining by DAPI. A merged panel is also given. (b) Respective % cell viability.

loaded PDMS hydrogel was taken as a negative control. From the figure it is observed that more profound bactericidal activity was observed in the case of the Gram positive bacteria as compared to the Gram negative bacteria. A significant zone of inhibition was shown by the curcumin loaded hydrogel sample in the case of both *S. aureus* (17 ± 1.5) mm and *E. coli* (14 ± 0.5) mm. Fig. 8c shows a graphical representation of the zone of inhibition that was created by the hydrogel. The morphological behavior of both *S. aureus* (Fig. 8d and e) and *E. coli* (Fig. 8f and g) bacteria after the treatment with curcumin was observed and it was found that the integrity of the smooth bacterial cell wall ruptured in the presence of curcumin molecules. In general *E. coli* has a rod like structure, whereas *S. aureus* has an elliptical cell morphology. Due to the leakage of the intercellular fluid, the cell wall of both the bacteria *S. aureus* and *E. coli* becomes wrinkled.[54,55] The antibacterial action of the curcumin is mainly observed due to the inhibition ability of the FtsZ protein formation in the bacterial body by curcumin. FtsZ is a protein encoded by the ftsZ gene which is important for bacterial cell division and viability. It is also a prokaryotic homologue of eukaryotic cytoskeletal protein tubulin. Curcumin mainly interrupts the FtsZ function, which indeed inhibits bacterial proliferation, resulting in the antibacterial property of the curcumin molecules.[56,57]

3.6. MTT colorimetric assay

To get an impression about the cytocompatibility of the curcumin loaded hydrogel and the pristine hydrogel, MTT colorimetric assay has been carried out against both the human dermal fibroblast cell line (Fig. 9) and the HaCat cell line (Fig. 10). It has been found that even up to a concentration of 50 μg ml^{-1}, both the curcumin loaded hydrogel and the pristine hydrogel are non-toxic to human dermal fibroblast cells as well as HaCat cells. One interesting phenomenon was observed that in the presence of curcumin the cell viability was higher as compared to the pristine hydrogel. This might be due to the high cell proliferation ability of curcumin.[56]

4. Conclusion

In conclusion, we have prepared a smart self-healable hydrogel based on a derivative of PDMS which can inhibit protein adhesion (antifouling activity) and also can be catastrophic against Gram-positive and Gram-negative bacteria. The as prepared hydrogel consists of amine modified PDMS based polymersomes which were crosslinked with an aldehyde modified PEG moiety *via* a Schiff-base reaction, a biocompatible reaction. To impart antifouling and antimicrobial activities into the hydrogel, a curcumin loaded PDMS based polyzwitterionic polymersome moiety was incorporated into the hydrogel formulation. It was observed that the formulated PDMS based hydrogel was able to sustained delivery of the drug curcumin for more than 72 h. Interestingly, the hydrogel can show self-healing behavior in the presence of saline solution *via* formation of ionic interlocking between the poly(zwitterionic) segments. This type of PDMS based smart hydrogel formulation can pave a new direction in therapeutic contact lens applications to cure several eye diseases.

Conflicts of interest

There are no conflicts to declare.

Acknowledgements

Funding for Mr Sovan Lal Banerjee's fellowship was kindly provided by IIT Kharagpur. Financial support from the Department of Science and Technology (DST) under the DST-DFG program (INT/FRG/DFG/P-04/2017) is gratefully acknowledged.

Notes and references

1 M. Van Beek, A. Weeks, L. Jones and H. Sheardown, Immobilized hyaluronic acid containing model silicone hydrogels reduce protein adsorption, *J. Biomater. Sci., Polym. Ed.*, 2008, **19**(11), 1425–1436.
2 E. García-Millán, S. Koprivnik and F. J. Otero-Espinar, Drug loading optimization and extended drug delivery of corticoids from pHEMA based soft contact lenses hydrogels via chemical and microstructural modifications, *Int. J. Pharm.*, 2015, **487**(1–2), 260–269.
3 O. Wichterle and D. Lim, Hydrophilic gels for biological use, *Nature*, 1960, **185**(4706), 117.
4 P. C. Nicolson and J. Vogt, Soft contact lens polymers: an evolution, *Biomaterials*, 2001, **22**(24), 3273–3283.
5 X. Duan and H. Sheardown, Dendrimer crosslinked collagen as a corneal tissue engineering scaffold: mechanical properties and corneal epithelial cell interactions, *Biomaterials*, 2006, **27**(26), 4608–4617.
6 Y.-C. Liu, T. T. Wong and J. S. Mehta, Intraocular lens as a drug delivery reservoir, *Curr. Opin. Ophthalmol.*, 2013, **24**(1), 53–59.
7 J. Kim, A. Conway and A. Chauhan, Extended delivery of ophthalmic drugs by silicone hydrogel contact lenses, *Biomaterials*, 2008, **29**(14), 2259–2269.
8 D. C. Chang, G. B. Grant, K. O'Donnell, K. A. Wannemuehler, J. Noble-Wang, C. Y. Rao, L. M. Jacobson, C. S. Crowell, R. S. Sneed and F. M. Lewis, Multistate outbreak of Fusarium keratitis associated with use of a contact lens solution, *JAMA*, 2006, **296**(8), 953–963.
9 L. Xie, W. Zhong, W. Shi and S. Sun, Spectrum of fungal keratitis in north China, *Ophthalmology*, 2006, **113**(11), 1943–1948.
10 N. V. Prajna, J. Mascarenhas, T. Krishnan, P. R. Reddy, L. Prajna, M. Srinivasan, C. Vaitilingam, K. C. Hong, S. M. Lee and S. D. McLeod, Comparison of natamycin and voriconazole for the treatment of fungal keratitis, *Arch. Ophthalmol.*, 2010, **128**(6), 672–678.
11 X. Hu, L. Hao, H. Wang, X. Yang, G. Zhang, G. Wang and X. Zhang, Hydrogel contact lens for extended delivery of ophthalmic drugs, *Int. J. Polym. Sci.*, 2011, **2011**, 814163.

12 D. Lee, S. Cho, H. S. Park and I. Kwon, Ocular Drug Delivery through pHEMA-Hydrogel Contact Lenses Co-Loaded with Lipophilic Vitamins, *Sci. Rep.*, 2016, **6**, 34194.
13 D. Luensmann and L. Jones, Protein deposition on contact lenses: the past, the present, and the future, *Cont. Lens Anterior Eye*, 2012, **35**(2), 53–64.
14 C.-H. Lin, H.-L. Cho, Y.-H. Yeh and M.-C. Yang, Improvement of the surface wettability of silicone hydrogel contact lenses via layer-by-layer self-assembly technique, *Colloids Surf., B*, 2015, **136**, 735–743.
15 D. Bozukova, C. Pagnoulle, M.-C. De Pauw-Gillet, S. Desbief, R. Lazzaroni, N. Ruth, R. Jérôme and C. Jérôme, Improved performances of intraocular lenses by poly (ethylene glycol) chemical coatings, *Biomacromolecules*, 2007, **8**(8), 2379–2387.
16 H. Chen, M. A. Brook, Y. Chen and H. Sheardown, Surface properties of PEO–silicone composites: reducing protein adsorption, *J. Biomater. Sci., Polym. Ed.*, 2005, **16**(4), 531–548.
17 J.-F. Huang, J. Zhong, G.-P. Chen, Z.-T. Lin, Y. Deng, Y.-L. Liu, P.-Y. Cao, B. Wang, Y. Wei and T. Wu, A hydrogel-based hybrid theranostic contact lens for fungal keratitis, *ACS Nano*, 2016, **10**(7), 6464–6473.
18 I. Banerjee, R. C. Pangule and R. S. Kane, Antifouling coatings: recent developments in the design of surfaces that prevent fouling by proteins, bacteria, and marine organisms, *Adv. Mater.*, 2011, **23**(6), 690–718.
19 D. Hong, H.-C. Hung, K. Wu, X. Lin, F. Sun, P. Zhang, S. Liu, K. E. Cook and S. Jiang, Achieving ultralow fouling under ambient conditions via surface-initiated arget atrp of carboxybetaine, *ACS Appl. Mater. Interfaces*, 2017, **9**(11), 9255–9259.
20 H. Lísalová, E. Brynda, M. Houska, I. Visova, K. Mrkvova, X. C. Song, E. Gedeonova, F. Surman, T. Riedel and O. Pop-Georgievski, Ultralow-Fouling Behavior of Biorecognition Coatings Based on Carboxy-Functional Brushes of Zwitterionic Homo-and Copolymers in Blood Plasma: Functionalization Matters, *Anal. Chem.*, 2017, **89**(6), 3524–3531.
21 K. M. Nelson, J. L. Dahlin, J. Bisson, J. Graham, G. F. Pauli and M. A. Walters, The essential medicinal chemistry of curcumin: miniperspective, *J. Med. Chem.*, 2017, **60**(5), 1620–1637.
22 A. B. Sharangi, *Indian Spices: The Legacy, Production and Processing of India's Treasured Export*, Springer, 2018.
23 X.-F. Liu, J.-L. Hao, T. Xie, N. J. Mukhtar, W. Zhang, T. H. Malik, C.-W. Lu and D.-D. Zhou, Curcumin, a potential therapeutic candidate for anterior segment eye diseases: a review, *Front. Pharmacol.*, 2017, **8**, 66.
24 B. M. Discher, Y.-Y. Won, D. S. Ege, J. C. Lee, F. S. Bates, D. E. Discher and D. A. Hammer, Polymersomes: tough vesicles made from diblock copolymers, *Science*, 1999, **284**(5417), 1143–1146.
25 B. M. Discher, H. Bermudez, D. A. Hammer, D. E. Discher, Y.-Y. Won and F. S. Bates, Cross-linked polymersome membranes: vesicles with broadly adjustable properties, *J. Phys. Chem. B*, 2002, **106**(11), 2848–2854.
26 S. L. Banerjee and N. K. Singha, A new class of dual responsive self-healable hydrogels based on a core crosslinked ionic block copolymer micelle prepared via RAFT polymerization and Diels–Alder "click" chemistry, *Soft Matter*, 2017, **13**(47), 9024–9035.
27 Y.-L. Liu and T.-W. Chuo, Self-healing polymers based on thermally reversible Diels–Alder chemistry, *Polym. Chem.*, 2013, **4**(7), 2194–2205.
28 S. L. Banerjee, K. Bhattacharya, S. Samanta and N. K. Singha, Self-Healable Antifouling Zwitterionic Hydrogel Based on Synergistic Phototriggered Dynamic Disulfide Metathesis Reaction and Ionic Interaction, *ACS Appl. Mater. Interfaces*, 2018, **10**(32), 27391–27406.
29 J. Canadell, H. Goossens and B. Klumperman, Self-healing materials based on disulfide links, *Macromolecules*, 2011, **44**(8), 2536–2541.
30 S. L. Banerjee, R. Hoskins, T. Swift, S. Rimmer and N. K. Singha, A self-healable fluorescence active hydrogel based on ionic block copolymers prepared via ring opening polymerization and xanthate mediated RAFT polymerization, *Polym. Chem.*, 2018, **9**(10), 1190–1205.
31 M. H. Stenzel, L. Cummins, G. E. Roberts, T. P. Davis, P. Vana and C. Barner-Kowollik, Xanthate mediated living polymerization of vinyl acetate: a systematic variation in MADIX/RAFT agent structure, *Macromol. Chem. Phys.*, 2003, **204**(9), 1160–1168.
32 V. K. Patel, A. K. Mishra, N. K. Vishwakarma, C. S. Biswas and B. Ray, S)-2-(Ethyl propionate)-(O-ethyl xanthate) and (S)-2-(Ethyl isobutyrate)-(O-ethyl xanthate)-mediated RAFT polymerization of N-vinylpyrrolidone, *Polym. Bull.*, 2010, **65**(2), 97–110.
33 A. K. Mishra, N. K. Vishwakarma, V. K. Patel, C. S. Biswas, T. K. Paira, T. K. Mandal, P. Maiti and B. Ray, Synthesis, characterization, and solution behavior of well-defined double hydrophilic linear amphiphilic poly (N-isopropylacrylamide)-*b*-poly (ε-caprolactone)-*b*-poly (N-isopropylacrylamide) triblock copolymers, *Colloid Polym. Sci.*, 2014, **292**(6), 1405–1418.
34 S. Perrier and P. Takolpuckdee, Macromolecular design via reversible addition–fragmentation chain transfer (RAFT)/xanthates (MADIX) polymerization, *J. Polym. Sci., Part A: Polym. Chem.*, 2005, **43**(22), 5347–5393.
35 W. Y. Seow, G. Salgado, E. B. Lane and C. A. Hauser, Transparent crosslinked ultrashort peptide hydrogel dressing with high shape-fidelity accelerates healing of full-thickness excision wounds, *Sci. Rep.*, 2016, **6**, 32670.
36 H. Saito, A. Sakurai, M. Sakakibara and H. Saga, Preparation and properties of transparent cellulose hydrogels, *J. Appl. Polym. Sci.*, 2003, **90**(11), 3020–3025.
37 G. Sun, Z. Li, R. Liang, L.-T. Weng and L. Zhang, Super stretchable hydrogel achieved by non-aggregated spherulites with diameters < 5 nm, *Nat. Commun.*, 2016, **7**, 12095.
38 R. Pan, G. Liu, Y. Li, Y. Wei, S. Li and L. Tao, Size-dependent endocytosis and a dynamic-release model of nanoparticles, *Nanoscale*, 2018, **10**(17), 8269–8274.
39 D. J. Haloi, P. Mandal and N. K. Singha, Atom transfer radical polymerization of glycidyl methacrylate (GMA) in emulsion, *J. Macromol. Sci., Part A: Pure Appl. Chem.*, 2013, **50**(1), 121–127.

40 J. Lee, J. Kim, H. Kim, Y. M. Bae, K.-H. Lee and H. J. Cho, Effect of thermal treatment on the chemical resistance of polydimethylsiloxane for microfluidic devices, *J. Micromech. Microeng.*, 2013, **23**(3), 035007.
41 Q. Zhang, Y. Liu, Y. Su, R. Zhang, L. Fan, Y. Liu, T. Ma and Z. Jiang, Fabrication and characterization of antifouling carbon nanotube/polyethersulfone ultrafiltration membranes, *RSC Adv.*, 2016, **6**(42), 35532–35538.
42 S. Yuan, J. Zhang, Z. Yang, S. Tang, B. Liang and S. O. Pehkonen, Click functionalization of poly (glycidyl methacrylate) microspheres with triazole-4-carboxylic acid for the effective adsorption of Pb (II) ions, *New J. Chem.*, 2017, **41**(14), 6475–6488.
43 J. B. You, K.-I. Min, B. Lee, D.-P. Kim and S. G. Im, A doubly cross-linked nano-adhesive for the reliable sealing of flexible microfluidic devices, *Lab Chip*, 2013, **13**(7), 1266–1272.
44 G. Gaucher, M.-H. Dufresne, V. P. Sant, N. Kang, D. Maysinger and J.-C. Leroux, Block copolymer micelles: preparation, characterization and application in drug delivery, *J. Controlled Release*, 2005, **109**(1–3), 169–188.
45 K. Kita-Tokarczyk, J. Grumelard, T. Haefele and W. Meier, Block copolymer vesicles—using concepts from polymer chemistry to mimic biomembranes, *Polymer*, 2005, **46**(11), 3540–3563.
46 Y. Chang, W. Yandi, W.-Y. Chen, Y.-J. Shih, C.-C. Yang, Y. Chang, Q.-D. Ling and A. Higuchi, Tunable bioadhesive copolymer hydrogels of thermoresponsive poly (N-isopropyl acrylamide) containing zwitterionic polysulfobetaine, *Biomacromolecules*, 2010, **11**(4), 1101–1110.
47 B. G. Choi, S.-H. Cho, H. Lee, M. H. Cha, K. Park, B. Jeong and D. K. Han, Thermoreversible radial growth of micellar assembly for hydrogel formation using zwitterionic oligopeptide copolymer, *Macromolecules*, 2011, **44**(7), 2269–2275.
48 C.-H. Lin, Y.-H. Yeh, W.-C. Lin and M.-C. Yang, Novel silicone hydrogel based on PDMS and PEGMA for contact lens application, *Colloids Surf., B*, 2014, **123**, 986–994.
49 Y. Zhang, L. Tao, S. Li and Y. Wei, Synthesis of multiresponsive and dynamic chitosan-based hydrogels for controlled release of bioactive molecules, *Biomacromolecules*, 2011, **12**(8), 2894–2901.
50 T. C. Tseng, L. Tao, F. Y. Hsieh, Y. Wei, I. M. Chiu and S. H. Hsu, An injectable, self-healing hydrogel to repair the central nervous system, *Adv. Mater.*, 2015, **27**(23), 3518–3524.
51 L. Jones and K. Dumbleton, Silicone hydrogel lenses: Fitting procedures and in-practice protocols for continuous wear lenses, *Optician*, 2002, **223**(5840), 37–45.
52 J. Wang, Z. Wang, J. Wang and S. Wang, Improving the water flux and bio-fouling resistance of reverse osmosis (RO) membrane through surface modification by zwitterionic polymer, *J. Membr. Sci.*, 2015, **493**, 188–199.
53 C. Leng, S. Sun, K. Zhang, S. Jiang and Z. Chen, Molecular level studies on interfacial hydration of zwitterionic and other antifouling polymers in situ, *Acta Biomater.*, 2016, **40**, 6–15.
54 X. Huang, X. Bao, Y. Liu, Z. Wang and Q. Hu, Catechol-functional chitosan/silver nanoparticle composite as a highly effective antibacterial agent with species-specific mechanisms, *Sci. Rep.*, 2017, **7**(1), 1860.
55 V. Gopinath, S. Priyadarshini, M. F. Loke, J. Arunkumar, E. Marsili, D. MubarakAli, P. Velusamy and J. Vadivelu, Biogenic synthesis, characterization of antibacterial silver nanoparticles and its cell cytotoxicity, *Arabian J. Chem.*, 2015, **10**(8), 1107–1117.
56 M. Khamrai, S. L. Banerjee and P. P. Kundu, Modified bacterial cellulose based self-healable polyeloctrolyte film for wound dressing application, *Carbohydr. Polym.*, 2017, **174**, 580–590.
57 S. Kaur, N. H. Modi, D. Panda and N. Roy, Probing the binding site of curcumin in Escherichia coli and Bacillus subtilis FtsZ–a structural insight to unveil antibacterial activity of curcumin, *Eur. J. Med. Chem.*, 2010, **45**(9), 4209–4214.